

# Dosimetric Approaches for Radioimmunotherapy of Non-Hodgkin Lymphoma in Myeloablative Setting

Francesco Cicone<sup>1,2</sup>, Anna Sarnelli<sup>3\*</sup>, Claretta Guidi<sup>3</sup>, Maria Luisa Belli<sup>3</sup>, Mahila Esmeralda Ferrari<sup>4</sup>,  
Richard Wahl<sup>5</sup>, Giovanni Paganelli<sup>7°</sup>, Marta Cremonesi<sup>6°</sup>

<sup>1</sup>Department of Experimental and Clinical Medicine, and Neuroscience Research Centre, PET/RM Unit, "Magna Graecia" University of Catanzaro, Catanzaro, Italy

<sup>2</sup>Nuclear Medicine Unit, University Hospital "Mater Domini", Catanzaro, Italy

<sup>3</sup>Medical Physics Unit, IRCCS Istituto Romagnolo per lo Studio dei Tumori (IRST) "Dino Amadori", Meldola, Italy

<sup>4</sup>Medical Physics, IEO European Institute of Oncology IRCCS, Milan, Italy

<sup>5</sup>Mallinckrodt Institute of Radiology, Washington University School of Medicine, St. Louis, MO 63130, USA

<sup>6</sup>Radiation Research Unit, IEO European Institute of Oncology IRCCS, Milan, Italy

<sup>7</sup>Nuclear Medicine Unit, IRCCS Istituto Romagnolo per lo Studio dei Tumori (IRST) "Dino Amadori", Meldola, Italy

\* Corresponding author: [anna.sarnelli@irst.emr.it](mailto:anna.sarnelli@irst.emr.it)

° These authors equally contributed as senior Authors, and therefore share co-last authorship

## 24 **Abstract**

25 Radioimmunotherapy (RIT) is a safe and active treatment available for non-Hodgkin lymphomas (NHLs). In  
26 particular, two monoclonal antibodies raised against CD20, i.e. Zevalin® (<sup>90</sup>Y-ibritumomab-tiuxetan) and  
27 Bexxar® (<sup>131</sup>I-tositumomab) received FDA approval for the treatment of relapsing/refractory indolent or  
28 transformed NHLs. RIT is likely the most effective and least toxic anticancer agent in NHLs. However, its use  
29 in the clinical setting is still debated and, in case of relapse after optimized rituximab-containing regimens,  
30 the efficacy of RIT at standard dosage is suboptimal. Thus, clinical trials were based on the hypothesis that  
31 the inclusion of RIT in myeloablative conditioning would allow to obtain improved efficacy and toxicity  
32 profiles when compared to myeloablative total-body irradiation and/or high-dose chemotherapy regimens.  
33 Standard-activity RIT has a safe toxicity profile, and the utility of pre-therapeutic dosimetry in this setting  
34 can be disputed. In contrast, dose-escalation clinical protocols require the assessment of  
35 radiopharmaceutical biodistribution and dosimetry before the therapeutic injection, as dose constrains for  
36 critical organs may be exceeded when RIT is administered at high activities .

37 The aim of the present study was to review and discuss the internal dosimetry protocols that were adopted  
38 for non-standard RIT administration in the myeloablative setting before hematopoietic stem cell  
39 transplantation in patients with NHLs.

40

# 41 1) Introduction

42 Mature lymphoid neoplasms comprise a number of malignant tumors of the lymphoid tissue that can be  
43 divided into three main categories: B-cell neoplasms, T-cell and NK-cell neoplasms, and Hodgkin's  
44 lymphomas (HL). Lymphomas other than HL are also commonly referred to as non-Hodgkin lymphomas  
45 (NHL). Overall, mature B-cell neoplasms account for >90% of all lymphoid neoplasms. Follicular lymphoma  
46 (FL) and Diffuse large B-cell lymphoma (DLBCL) are the most common types of lymphoma, representing  
47 about 60% of all NHLs<sup>1</sup>.

48 HL can be cured in most cases with a combination of chemotherapy and external beam radiotherapy  
49 (EBRT)<sup>2</sup>. In contrast, NHLs have heterogeneous clinical courses and prognosis, and their clinical  
50 management ranges from watchful waiting and/or localized EBRT to myeloablative, high dose  
51 chemotherapy (HD-CT) followed by autologous (auto-SCT, indicated also as ASCT) or allogenic (allo-SCT)  
52 stem cell transplantation<sup>3</sup>. Standard chemo-immunotherapies, although very active, are accompanied by  
53 adverse side effects in many cases<sup>4</sup>.

54 Among the treatment strategies available for NHLs there is the so called Radioimmunotherapy (RIT). In  
55 particular, two CD20-targeting radiolabelled full IgG antibodies, namely Zevalin® (<sup>90</sup>Y-ibritumomab-  
56 tiuxetan) and Bexxar® (<sup>131</sup>I-tositumomab) received FDA approval at the beginning of this century for the  
57 treatment of relapsing/refractory indolent or transformed NHLs. Zevalin® was also approved in Europe with  
58 the same clinical indications<sup>5,6,7</sup>. Ten years after FDA approval, in 2014, Bexxar® was withdrawn from the  
59 market for commercial reasons. In some countries, other CD-20 targeting RIT agents, such as <sup>131</sup>I-rituximab,  
60 were tested clinically<sup>8,9,10</sup>.

61 RIT is arguably the most effective and least toxic anticancer agent in NHLs. In patients with FL, 87% and 97%  
62 overall response rates (ORR), including 56% and 75% complete responses (CR), were obtained after a single  
63 frontline infusion of Zevalin® and Bexxar®, respectively<sup>11,12,13</sup>. However, in case of relapse after optimized  
64 rituximab-including treatments, the efficacy of RIT was reduced<sup>14,15</sup>.

65 RIT was tested in diverse clinical settings including, among the others, frontline (FL)<sup>11,12</sup>, consolidation of  
66 advanced-stage FL<sup>16,17</sup> or DLBCL<sup>18</sup>, salvage treatment for relapsing DLBCL<sup>19</sup> or, as part of conditioning  
67 regimens prior to SCT<sup>20</sup>. In the pre-transplant setting, RIT was given at standard<sup>21,22,23,24,25</sup> or increased  
68 activities<sup>26,27,28,29,30,31,32,33,34,35,36,37</sup>, with or without a combination of myeloablative chemo/radiotherapy.  
69 These clinical trials were based on the hypothesis that the inclusion of RIT in myeloablative conditioning,  
70 either at standard or at high injected activities, would show improved efficacy and toxicity profiles  
71 compared to classical myeloablative total-body irradiation (TBI) and/or high-dose chemotherapy  
72 regimens<sup>38,39,40</sup>.

73 Standard-activity RIT has a generally safe toxicity profile and the utility of pre-therapeutic dosimetry in this  
74 setting can be disputed. In contrast, dose-escalation clinical protocols require the assessment of  
75 radiopharmaceutical biodistribution and dosimetry before the therapeutic injection, as dose constrains  
76 may be exceeded for critical organs when RIT is administered at high activities<sup>41</sup>.

77 The aim of the present study was to review and discuss the internal dosimetry protocols that were adopted  
78 for non-standard RIT administration in the myeloablative setting before hematopoietic SCT in patients with  
79 NHLs.

80

## 81 **2) High-dose RIT in stem cell transplant conditioning: clinical** 82 **protocols and results**

83 Following the results of the PARMA study, bone marrow ablation followed by auto-SCT is the established  
84 standard-of-care for chemosensitive relapses of DLBCL<sup>42</sup>. For patients with refractory disease, or for  
85 patients who relapse after auto-SCT, allo-SCT can be considered as a curative option. In FL, auto-SCT is  
86 usually offered to patients relapsing after two or three previous lines of chemo - immunotherapies. The  
87 correct timing and indication to the use of allo-SCT in FL is controversial, although allo-SCT remains the only  
88 curative option for this disease<sup>43</sup>. The best conditioning regimen for either auto- or allo-SCT has not been  
89 established yet, and the choice might also be subject to local availability of chemotherapeutics<sup>44,45,46</sup>. For  
90 the purpose of the present work, only studies including high-activity (or high-dose) RIT (HD-RIT) in SCT  
91 conditioning were reviewed. A summary of these studies is given in Table 1.

92

### 93 **Myeloablative radioimmunotherapy with <sup>131</sup>I-Bexxar® and <sup>131</sup>I-Rituximab.**

94 Press and co-workers pioneered the use of HD-RIT with anti-CD20 antibodies as conditioning regimen  
95 before auto-SCT. In their phase I study, patients with various relapsed B cell NHLs showing favourable  
96 Bexxar® biodistribution, defined as a dose to the tumor higher than that of the liver, lung and kidneys, were  
97 treated with dose escalated Bexxar® (at that time called <sup>131</sup>I-anti-B1). The protocol was designed to deliver  
98 from 16.75 up to 30.75 Gy to the dose-limiting organs, respectively<sup>47</sup>. Auto-SCT was performed when  
99 radiation exposure was <0.02 mSv/h at 1 meter distance. Hematological toxicity was managed by stem cell  
100 rescue, and the study established that the administration of HD-RIT delivering more than 27 Gy to the  
101 dose-limiting organ, usually the lungs, was the toxicity limit. The ORR of 95%, including 84% CR, together  
102 with a median duration of response >11 months were considered very encouraging and prompted further

103 phase II studies designed to deliver between 25 and 31 Gy to the organ receiving the highest dose, which  
104 was most often the lungs or, occasionally, the kidneys. Projected 2-year overall survival (OS) and  
105 progression-free survival (PFS) were 93% and 62% respectively, with better PFS estimates obtained in  
106 patients receiving more than 20 Gy to the dose-limiting organ<sup>48</sup>. Further follow up analysis of the 29 treated  
107 patients showed 4-years projected OS and PFS of 68% and 42%, respectively. Early death occurred in two  
108 patients. Two patients developed second solid neoplasms; none developed myelodysplasia or acute  
109 leukemia. Late toxicities included chronic thrombocytopenia (n=1), hepatitis (n=1), chronic renal (n=1),  
110 cardiac (n=1) and pulmonary (n=2) insufficiency. Elevation of TSH levels was observed in 60% of patients<sup>49</sup>.  
111 The strategy of delivering 25-27 Gy to the critical organ with HD-RIT Bexxar<sup>®</sup> followed by auto-SCT proved  
112 to be safe in patients older than 60 years (median age 64 years, range: 60-76 years) as well, with no  
113 treatment-related mortality and only two grade 4 non-haematological toxicities in 24 treated patients.  
114 Survival outcomes in this fragile patient population were also satisfactory, with 3-year estimated OS and  
115 PFS of 59% and 51%, respectively<sup>27</sup>.

116 The same group in Seattle, designed a trial to establish the maximum tolerated absorbed dose of Bexxar<sup>®</sup>  
117 to be safely combined with high-dose etoposide (60 mg/kg) and cyclophosphamide (100 mg/kg) followed  
118 by auto-SCT for the treatment of patient with relapsed CD20-positive NHLs. Fifty-two patients (n=38 FL, n=8  
119 de novo or transformed DLBCL, n=6 mantle cell lymphomas (MCL)) were divided in four groups, receiving  
120 20, 23, 25 and 27 Gy to the dose-limiting organ, respectively, in addition to high-dose chemotherapy. The  
121 highest dose level of 27 Gy proved to be excessively toxic, with three life-threatening events occurring in 8  
122 patients including one death. Therefore the maximum tolerated dose delivered by Bexxar<sup>®</sup> in this setting  
123 was considered to be 25 Gy to the dose-limiting organ. Two-year projected OS and PFS were 83% and 68%,  
124 respectively, which resulted significantly advantageous over historical controls treated with TBI-including  
125 conditioning<sup>50</sup>. The 10-year follow-up results of this conditioning regimen in 101 treated patients showed  
126 62%, 64% and 43% PFS in n=29 aggressive NHLs, n=45 indolent NHLs, and n=33 MCL, respectively, with  
127 2.8% non-relapse mortality at 100 days<sup>36</sup>.

128 HD-RIT with Bexxar<sup>®</sup> delivering up to 27 Gy to the critical organ was tested in combination with escalating  
129 dosages of fludarabine prior to auto-STC in 36 patients older than 60 years (median: 65 years, range: 60-76)  
130 with relapsing/refractory B cell NHLs, including n=23 MCL and n=8 de novo or transformed DLBCL. No  
131 treatment-related deaths were observed, and grade 4 non-haematological toxicities were observed in 2  
132 patients only. Three-year estimated OS and PFS were 54% and 53%, respectively<sup>28</sup>.

133 Additionally, the anti-CD20 antibody Rituximab was radiolabeled with <sup>131</sup>I and used in some countries<sup>8,9,10</sup>.  
134 <sup>131</sup>I-Rituximab was tested with various combinations of high-dose chemotherapy as auto-SCT conditioning.  
135 Results of the first two original reports, obtained in a small number of patients, were encouraging in terms  
136 of survival outcomes, but showed significant toxicities<sup>33,35</sup>.

137

138 **Myeloablative radioimmunotherapy with <sup>90</sup>Y-Zevalin®.**

139 The inclusion of HD-RIT with Zevalin® in auto-SCT conditioning was firstly adopted by Nademanee et al. in  
140 patients with poor-risk or recurrent CD20-positive B-cell NHL, including FL, DLBCL and MCL<sup>29</sup>. Patients were  
141 ruled out if the tumor dose was inferior to that of any other organ excluding spleen and bone marrow,  
142 unless patients were in complete remission (CR) at the time of treatment. The activity to be administered  
143 was designed to deliver a maximum of 10 Gy to any organ excluding the spleen and the bone marrow, with  
144 a pre-determined maximum limit of 3.7 GBq. A median activity of 2.7 GBq Zevalin® was injected at day -14,  
145 followed by high-dose etoposide and cyclophosphamide. Autologous stem cells were reinfused at day +1,  
146 unless the bone marrow absorbed dose was determined to be >50 mGy. Of the 41 patients enrolled, 31  
147 underwent the full therapeutic procedure. The treatment resulted in satisfactory 2-year survival outcomes,  
148 and the toxicity profiles observed, with 3% transplantation-related mortality, were similar to historical  
149 controls using TBI in addition to high-dose etoposide and cyclophosphamide MCL<sup>29</sup>.

150 A different strategy was pursued by Ferrucci et al.<sup>31</sup> at IEO in Milan. The Authors demonstrated feasibility  
151 and safety of auto-SCT conditioning based on HD-RIT with Zevalin® alone in NHL patients unfit for high-dose  
152 chemotherapy because of age or co-morbidities. Thirteen patients (median age: 68 years) with  
153 refractory/transformed B-cell NHL (n=8 DLBCL, n=3 MCL, n=1 FL and n=1 marginal lymphoma) were divided  
154 in three groups receiving 30 MBq/kg, 45 MBq/kg or 56 MBq/kg, respectively. Autologous stem cells were  
155 reinfused at day +13. Based on dosimetry, two patients were assigned to activity levels lower than initially  
156 planned without personalized dosimetric data. Similarly, bone marrow engraftment was delayed in one  
157 patient treated with the highest activity schedule. A trend towards higher haematological toxicity was  
158 found in patients with more than three previous lines of chemotherapy and reduced bone marrow reserve.  
159 One heavily pre-treated patient developed a myelodysplastic syndrome two years after treatment while  
160 being in continuous CR. Acute non-haematological toxicities were manageable in all cases.

161 Devizzi et al.<sup>32</sup> enrolled 30 patients (median age: 62 years) with various CD20-positive NHLs (including,  
162 among the others, n=10 DLBCL, n=12 FL and n=3 MCL) who underwent induction chemotherapy and stem  
163 cell harvesting, followed by a single consolidation treatment with HD-RIT Zevalin® before auto-SCT. Most  
164 patients (n=19) were ineligible for conventional autografting. Zevalin® was given at 30 MBq/kg or 45  
165 MBq/kg in n=17 and n=13 patients, respectively, followed by two tandem infusions of autologous stem  
166 cells, on day +7 and +14, respectively. Neutrophil and platelets counts fully recovered 7 and 14 days after  
167 auto-SCT, respectively. No non-haematological toxicities greater than grade 3 were observed. In the overall  
168 population, 30-month projected OS and event-free survival were 87% and 69%, respectively<sup>32</sup>.

169 Winter et al. showed the feasibility and the safety of combining dose-escalated Zevalin® with high-dose  
170 BEAM (carmustine, etoposide, cytarabine and melphalan) conditioning before auto-SCT in 44 patients with  
171 relapsing/refractory CD20-positive NHLs (n=33 de novo or transformed DLBCL, n=4 FL, n=7 MCL), including  
172 30% of patients who had achieved less than a partial remission after their most recent salvage therapy, and  
173 would have been considered non-eligible for auto-SCT<sup>30</sup>. Administered therapeutic activities of Zevalin®  
174 were targeted to deliver increasing absorbed doses (range 1-17 Gy) to the critical organs. There were two  
175 dose-limiting non-haematological toxicities including one patient death of septic pneumonia at the 17 Gy  
176 dose level, therefore the maximum tolerated absorbed dose to the critical organ (liver) was set at 15 Gy.  
177 Additional grade 4 toxicities included infections, obstructive uropathy, pulmonary embolism, and veno-  
178 occlusive disease. Survival outcome profiles compared favourably to historical data of similar cohorts<sup>30</sup>.

179 More recently, Wahl and colleagues<sup>37</sup> proposed a hybrid approach (SPECT/CT and planar images) for  
180 dosimetry-based dose-escalated RIT with Zevalin® followed by auto-SCT in 18 patients with chemo sensitive  
181 relapses of CD20-positive NHLs. Patients were divided into four groups, targeted to receive 18, 24, 28 and  
182 30.5 Gy to the liver, respectively. Stem cells were infused when the predicted bone marrow dose rate was <  
183 10 mGy/h. Haematological toxicity was mild and reversible. No liver toxicity was observed. One patient died  
184 of pneumonia 27 days after auto-SCT. The study showed that a dosimetry-based protocol could safely  
185 deliver Zevalin® activities up to five times higher than the maximum prescribed standard. Unfortunately,  
186 the study was terminated prematurely for commercial reasons and only one patient could be enrolled at  
187 the highest dose level of 30.5 Gy and the maximum tolerated dose could not be established. Response  
188 rates were encouraging (88% ORR, with 13 CR and 3 PR), although of short duration, and no correlation was  
189 shown with the Zevalin® administered activity<sup>37</sup>.

190 HD-RIT Zevalin® was also tested as part of reduced intensity conditioning (RIC) before allo-SCT in 20  
191 patients with aggressive CD20-positive NHLs with a median of four previous therapy courses including auto-  
192 SCT<sup>34</sup>. Patients were assigned receive either 22 MBq/kg (n=10) or 30 MBq/kg (n=10) Zevalin® at day -14,  
193 followed by fludarabine, melphalan and alemtuzumab before allo-SCT at day 0. Non-relapse mortality was  
194 0% at day 100, and 30% at 3 years. The authors concluded that these features do not represent an  
195 increased toxicity compared to RIC without RIT in patients with these characteristics<sup>34</sup>.

196

### 197 **3) Dosimetry protocols**

198 In the myeloablative RIT setting, several dosimetric protocols were adopted, depending both on the  
199 radiopharmaceutical characteristics and on the specific authors' approach. All of these protocols refer to  
200 the widely accepted MIRD approach<sup>51,52</sup>. Most protocols are based on the whole body planar images (two-

201 dimensional, 2D) acquired at different time points post tracer injection (p.i.)<sup>51,52</sup>. The MIRD 16 pamphlet  
202 suggests to improve the accuracy of activity measurements by correcting 2D-images for several factors  
203 (geometric mean of anterior and posterior view, background, attenuation, scattering etc.) however, no  
204 standard protocol including such corrections has been defined<sup>51,53</sup>. Moreover, the 2D approach presents  
205 several pitfalls, such as overlapping of structures, partial volume effect and uncertainties contouring the  
206 region of interest<sup>53</sup>. For these reasons, several studies promote hybrid or full three-dimensional (3D)  
207 protocols based on SPECT/CT<sup>37,53,54,55</sup>.

208 In myeloablative RIT, bone marrow suppression represents the wanted treatment effect. Consequently,  
209 dosimetry evaluations focused mostly on secondary critical organs. Nevertheless, bone marrow dosimetry  
210 can be used to identify the adequate time for SCT ensuring cell engraftment<sup>47,29,37</sup>. Appendix A summarizes  
211 the different bone marrow dosimetry approaches reported in literature. Owing to the large interpatient  
212 variability of normal tissues dosimetry, in myeloablative RIT it is not possible to identify a safe maximal  
213 activity to be administered or a single dose-limiting organ for all patients. Therefore, an individual  
214 dosimetry approach is suggested<sup>31,32,37,56,57,58,30</sup>. In the following, the main dosimetry protocols adopted with  
215 either <sup>90</sup>Y-Zevalin® or <sup>131</sup>I-labelled anti-CD20 antibodies Bexxar® and Rituximab are detailed.

216 A summary of the previsional dosimetry methods used by different authors for NHL RIT is reported in Table  
217 2.

218

### 219 **Studies with <sup>131</sup>I-labelled antibodies.**

220 To perform previsional dosimetry studies of Bexxar® and/or <sup>131</sup>I-rituximab, a tracer amount of the same  
221 therapeutic radiopharmaceutical is used, owing to the gamma emissions of <sup>131</sup>I. Given the highly  
222 penetrating <sup>131</sup>I gamma radiation which is easily detectable by thyroid probe or gamma scintigraphy, whole  
223 body radiation dose has been suggested to replace red marrow constraints. For previsional dosimetry,  
224 tracing activities of <sup>131</sup>I-Bexxar® or <sup>131</sup>I-rituximab are measured longitudinally after pre-loading with the cold  
225 antibodies tositumomab and rituximab, respectively. In their early studies with Bexxar®, Wahl and co-  
226 workers proposed a whole-body dosimetry approach based on sequential thyroid NaI probe  
227 measurements, which was later replaced by sequential gamma-camera imaging<sup>59</sup>. The dosimetric protocol  
228 based on the thyroid probe counting consisted of six or more time-points measurements over 5-8 days,  
229 while the imaging-based protocol consisted of whole-body planar scans acquired at three time points over  
230 6-7 days. The conjugate-view method was used to calculate the total body count at each time point,  
231 corrected for the background contribution. No information about other corrections was reported. The main  
232 assumption of the whole body approach is that the radiopharmaceutical remained uniformly distributed  
233 throughout the patient's body after the injection. For standard RIT treatments, the activity to be



234 administered was targeted at delivering a total-body dose of 0.75 or 0.65 Gy in patients with platelet count  
235  $\geq$  or  $\leq$  150000/ml, respectively<sup>59,60</sup>.

236 In the dose escalation study described by Press and co-workers, the dosimetric protocol consisted of  
237 sequential whole body images acquired at 0, 48, 96 and 120 h post injection; no information were reported  
238 about the corrections applied<sup>47</sup>. In other studies of the same group, quantitative <sup>131</sup>I imaging was  
239 performed daily for seven days and data were corrected for whole body thickness, attenuation, radioactive  
240 decay, and electronic drift<sup>61,62</sup>.

241 The same approach was adopted with minor variations in all later HD-RIT studies performed by the same  
242 group (Table 2) Image-based dosimetry was used to determine the administered Bexxar® activity to deliver  
243 absorbed doses in the range of 25-31 Gy to the organ receiving the greatest dose (lungs, liver or kidneys),  
244 depending on the high-dose chemotherapy conditioning regimen used in combination with HD-RIT. SCT  
245 was performed when whole-body radiation exposure was  $<0.02$  mSv/h at 1 meter distance<sup>48,50,27,28,36</sup>.

246 Dosimetry of standard-activity <sup>131</sup>I-rituximab consisted of sequential whole-body scans acquired 1h, 4 and 7  
247 days p.i. to determine the effective half-life of the radiopharmaceutical. Some patients were enrolled in  
248 more extended hybrid dosimetry protocols including the acquisition of a single SPECT/CT scan at 5-7 p.i., or  
249 3D dosimetry after therapy based on SPECT/CT acquisitions. The whole-body clearance rate and the lean  
250 body weight were used to determine the injected activity to deliver 0.75 Gy to the whole-body, which  
251 ensured that red marrow dose never exceeded 2 Gy<sup>55</sup>.

252 Dose calculations were based on the two following assumptions: a) the activity concentration (activity/kg)  
253 based on the lean body weight is the same as the activity concentration in red marrow and b) the whole-  
254 body and red marrow residence times are equal. The Bolch et al.<sup>63</sup> approach was used to compute energy-  
255 dependent absorbed fractions for red marrow since the approach proposed in MIRDOSE3 underestimates  
256 the absorbed fractions for low electron energies. Therefore, the red marrow self-dose included <sup>131</sup>I  
257 contributions from both the non-penetrating absorbed fraction in the spine and that from photons, taking  
258 into account the expected cellularity fraction in the spine.

259 Hohloch and co-workers treated nine patients with myeloablative BEAM chemotherapy plus auto-SCT,  
260 followed by dose-escalated HD-RIT with <sup>131</sup>I-rituximab rescued by a second auto-SCT<sup>33</sup>. After the first auto-  
261 SCT, patient-specific dosimetry was performed to individualize the injected activities in order to keep  
262 kidney and lung absorbed doses below 25 Gy. Serial planar scans were acquired at different times points  
263 p.i. however, the corrections performed were not specified (Table 2). Red marrow dosimetry was based on  
264 the blood method<sup>64</sup>, assuming a non specific uptake<sup>65</sup>. The second SCT was performed after the total body  
265 activity of the patients had decreased to  $< 555$  MBq (20 days p.i., on average)<sup>33</sup>.

266 Wagner and co-workers performed a phase I/II study escalating  $^{131}\text{I}$ -rituximab injected activities to target  
267 the kidneys up to 27 Gy in combination with different high-dose chemotherapy protocols and auto-SCT<sup>35</sup>.  
268 For dosimetry evaluations the conjugate-view technique suggested by MIRD was applied, and planar scans  
269 were acquired up to 168 hours p.i. The corrections applied, as well as the method for organ segmentation  
270 were not reported<sup>35</sup>.

271

272

### 273 **Studies with $^{90}\text{Y}$ -Zevalin.**

274 Dosimetry protocols of  $^{90}\text{Y}$ -Zevalin<sup>®</sup> were based on the injection of tracing amounts (185 MBq) of the  
275 surrogate radiopharmaceutical  $^{111}\text{In}$ -tositumomab tiuxetan, after pre-loading with the anti-CD20 cold  
276 antibody rituximab (Mabthera<sup>®</sup>), 250 mg/m<sup>2</sup><sup>58</sup>.

277 In the Wiseman protocol<sup>58</sup>, serial whole body scans were acquired up to 6 days p.i. Attenuation correction  
278 was applied by using an average correction factor estimated from the first whole body image. No further  
279 corrections other than individual organ masses (measured from CT scans) were applied. The conjugate-view  
280 method was applied to estimate the activity concentration in lung, liver, spleen, kidney, and bone marrow.  
281 The absorbed doses evaluation was performed using the MIRDOSE 3.1 software. Dose to the red marrow  
282 was estimated by using both the Sgouros blood-based method<sup>64</sup> and the sacral image-derived method<sup>66</sup>,  
283 using patient-specific red marrow masses. Median absorbed doses to the patients resulted well below  
284 protocol-defined maximum limits (3 Gy to red marrow and 20 Gy to other organs), with spleen receiving  
285 the highest dose (7.4 Gy). No toxicities were observed lungs and kidneys; hepatic dysfunction was detected  
286 in a few patients, but attributed to other factors than RIT. Hematologic toxicity was reversible and transient  
287 and the maximum tolerated activity without SCT was set at 1.85 GBq<sup>58</sup>.

288 A different protocol was adopted by Nadamane et al. in their phase I/II trial using HD-RIT with Zevalin<sup>®</sup>  
289 combined with high-dose etoposide and cyclophosphamide, followed by auto-SCT<sup>29</sup>. For dosimetry, a  
290 hybrid approach was adopted, with serial planar images up to 144 h p.i. and two SPECT images at 4, 47-72 h  
291 p.i. No other corrections were specified. Blood samples were collected at 2, 4-6 h p.i. and at the same  
292 planar image timing to determine antibody clearance and red marrow absorbed dose. However, after the  
293 therapeutic injection, the biopsy method<sup>64</sup> (see the specific paragraph below) was adopted to estimate the  
294 actual dose and the correct timing for SCT, given a constraint of  $\leq 50$  mGy to the red marrow. Liver was the  
295 main organ at risk<sup>29</sup>.

296 A similar constraint on SCT timing (RM dose  $< 50$  mGy) was adopted by Cremonesi et al.<sup>56</sup>, while Chiesa et  
297 al.<sup>32,57</sup> verified this condition before performing the second ASCT in a TANDEM reinfusion approach. These  
298 authors adopted a planar-only approach with a different image acquisition timing (Table 2). Since bone

299 marrow trephine biopsies were negative, red marrow dosimetry was performed based on the blood  
300 model<sup>64</sup>. The attenuation correction was performed using a transmission scan with a <sup>57</sup>Co source. Images  
301 were also corrected for scatter and background with two different approaches. Chiesa et al. adopted the  
302 pseudo-extrapolation number method<sup>51</sup> for scatter correction instead of the energy windows method used  
303 by Cremonesi et al.<sup>56</sup>. For the background correction, Cremonesi et al.<sup>56</sup> performed an integral subtraction,  
304 while Chiesa et al. a partial subtraction only, based on the Bujis method<sup>67</sup>. The main role of dosimetry in  
305 these studies was to prevent toxicity verifying that dose constraints were respected. In particular,  
306 Cremonesi et al assumed a dose constraint of 20 Gy to organs-at-risk excluding the red marrow. As in the  
307 work of Nadamane et al.<sup>29</sup>, the liver was identified as the main organ at risk<sup>56,57</sup>.

308 In the phase I study of Winter et al. combining HD-RIT with BEAM chemotherapy before auto-SCT, different  
309 activities of Zevalin<sup>®</sup> were injected to deliver absorbed doses to critical organs ranging from 1Gy to 17Gy.  
310 The dosimetry was based on serial planar scans acquired up to 144h p.i.(Table 2). The same corrections  
311 reported by Wiseman et al were applied<sup>58</sup>. The recommended maximum tolerated dose to critical organs  
312 was finally set at 15 Gy. The main critical organ was the liver in all patients but four for whom it was the  
313 kidney<sup>30</sup>.

314 A similar approach based on dose constraints was recently adopted by Whal et al.<sup>37</sup>, who proposed a  
315 patient-specific, dosimetry-driven absorbed dose escalation allowing the adjustment of the injected activity  
316 as a function of different absorbed dose to the liver. For this reason, the accuracy of the dosimetry was a  
317 major focus in this study. In each patient, the authors implemented a hybrid dosimetric approach based on  
318 both serial planar and one SPECT/CT images. The SPECT/CT was used to rescale the time-activity curve  
319 derived from planar images and to calculate both the attenuation correction factors and patient specific  
320 organ masses. Both blood and image based methods were implemented for red marrow dosimetry. Even in  
321 this protocol, the red marrow dosimetry was used to estimate the appropriated time for stem cells  
322 infusion, defined at a red marrow dose rate < 10 mGy/h (Figure 3).

323 In the study of Bethge et al.<sup>34</sup> combining HD-RIT with RIC before allo-SCT, Zevalin<sup>®</sup> injected activities were  
324 escalated empirically, and not based on dosimetry. Nevertheless, sequential whole-body scans were  
325 acquired up to 6 days following the injection of <sup>111</sup>In-ibritumomab tiuxetan. The study does not specify  
326 whether corrections were applied, or if individual organ masses were calculated.

## 327 **4) Evolution of Dosimetric approaches for red marrow** 328 **dosimetry**

329

330 The bone marrow architecture is complex, therefore several bone marrow dosimetry models with varying  
331 degrees of complexity were developed over the years. So far, more refined bone marrow-specific  
332 dosimetry models have failed to show a clear superiority over simpler ones as regards dose/response  
333 correlations. Under the assumption of non-specific uptake, Sgouros et al.<sup>64</sup> was the first to focus on red  
334 marrow dose models in RIT, based on either blood samples collection or bone marrow biopsies. The  
335 method based on biopsy sampling is considered the gold standard but it implies high patient compliance  
336 and high expertise for activity measurements and specific corrections for each biopsy component (See  
337 details in the Appendix). The blood-based method is simpler, and allows to estimate the red marrow dose  
338 assuming an equal activity concentration in both plasma and the extracellular fluid volume.

339 Ferrer et al.<sup>68</sup> highlighted the importance of considering the specific red marrow uptake also in case of  
340 limited bone marrow disease in NHL patients treated with the anti CD22 antibody <sup>90</sup>Y-epratuzumab-  
341 tetraxetan. The authors compared the blood-based method (with rescaling for the patient-specific  
342 haematocrit) with an image-based approach that quantifies the uptake in L2-L4 vertebrae, under the  
343 assumption that the red marrow mass in L2-L4 is 6.7% of the total red marrow mass. Image-to-blood dose  
344 ratios of 2 were found, on average<sup>68</sup> (Figure 2). Dose results from image-based methodology were able to  
345 predict the haematological toxicity observed better than blood-based methods.

346 All the above described methods assume a red marrow homogeneous distribution. The data from a single  
347 region (either blood sample, single biopsy or imaged bone region) are considered adequate to represent  
348 the whole red marrow dose estimation. However, inter- and intra-patients differences in red marrow  
349 distribution may occur and largely impact on dosimetry evaluation<sup>69,70,71,72</sup>. Sgouros et al.<sup>73</sup> demonstrated  
350 the importance of considering such variability, although for a different antibody (<sup>131</sup>I-labeled HuM195, Anti-  
351 CD33). In particular, some marrow regions were identified and the total dose to the red marrow was  
352 calculated using three different image-based approaches: a) assuming a red marrow homogeneous  
353 distribution; b) using a volume-weighted average of the local marrow cumulated activity concentration; c)  
354 using a weighted average absorbed dose of the considered regions. Large differences were observed  
355 among patients in all regions and results showed a large inter- and intra-patient variability, leading to the  
356 conclusion that a patient-specific approach is needed for a more accurate RM dose estimate (Figure 2).

357 The Sgouros' study<sup>73</sup> also shows the influence of different S-factors for red marrow self-irradiation in the  
358 dose evaluation. In fact, different models have been implemented over the years<sup>74</sup>. Spiers et al.<sup>75,76</sup>  
359 evaluated the dose conversion factors (DFs) for marrow irradiation by beta-emitting radionuclides within  
360 the trabecular bone by statistical evaluations of the electron path in experiments with trabecular bone  
361 samples. Cristy and Eckerman<sup>77</sup> improved the low-energy evaluations (previously underestimated),  
362 developed different phantoms, and provided regional and skeletal average dose conversion factors,  
363 implemented in the MIRDOSE3 software. Finally Bouchet et al.<sup>78</sup> developed a new model to generate S-

364 factor for 22 skeletal sites, employing a 3D Monte Carlo code (EGS4). However, the Eckerman model  
365 underestimated the absorbed fractions at photon energies < 200keV, while the Bouchet model  
366 overestimated these values at energies higher than 20keV. Thus, an adjusted model, combining the  
367 previous results at different energy ranges, was proposed<sup>79,80,81</sup>. Despite these efforts, we should point out  
368 that the improved S factors show a negligible impact on the red marrow dosimetry with respect to the  
369 influence related to the blood- or image-based dosimetric approach.

370

## 371 **5 Discussion**

372 Although direct comparisons in phase III randomized trials are not available, the use of HD-RIT in  
373 myeloablative conditioning seems to be less toxic than more used conditioning regimens based on high-  
374 dose chemotherapy and TBI. Ultimately, less toxicity is leading to improved survival outcomes<sup>39,40</sup>. Elderly  
375 or fragile patients, considered non-suitable for high-dose chemo/radiotherapy, were successfully treated  
376 with HD-RIT-based conditioning followed by SCT. In HD-RIT myeloablative protocols rescued by SCT, red  
377 marrow irradiation and/or toxicity is not the major concern. In contrast to standard-activity RIT, other  
378 organs become at risk. Due to the very high activities administered, dosimetry analysis was often included  
379 in HD-RIT clinical trials as a tool to establish the safe dose constraints allowing activity-escalation. In  
380 particular, the activity to be administered was calculated to accomplish specific dose limits to the organs  
381 receiving the highest dose, namely the lungs, the liver and the kidneys.

382 A summary of the most important clinical studies of HD-RIT followed by SCT is reported in Table 1. The  
383 experience gained from standard RIT was often a useful starting point to optimize the HD-RIT dosimetry  
384 methods in terms of acquisition timing, data collection and analysis. For this reason, we have also briefly  
385 summarized the dosimetry methods and some results of the most relevant studies using standard RIT  
386 (Table 2). The histograms in Figure 1 (a, b) report the median absorbed dose values for the most relevant  
387 organs obtained with either <sup>131</sup>I- or <sup>90</sup>Y-labelled radiopharmaceuticals. In case of escalation studies, the  
388 dose values reported refer to the group receiving the highest absorbed dose to the organ at risk or the  
389 highest activity/kg of body weight, according to the protocols' outlines summarised in Table 2. The various  
390 studies differ regarding the rationales, methodologies, activity levels, and dose constraints, which makes  
391 the comparison between the absorbed dose values reported in Figure 1 a difficult task. An actual  
392 dosimetry comparison should be based, instead, on absorbed dose per unit activity values. However, only  
393 few authors provided such information for organs other than the red marrow. A common evidence  
394 emerging from all studies is the large variability of the absorbed doses within the patient cohorts. Table 3  
395 reports the range of dose variability factors related to the major source organs, in terms of ratio between  
396 the minimum/maximum dose and the median dose (activity escalation protocols) or and the ratio between

397 the minimum/maximum activity and the median activity for a same dose constraint (dose escalation  
398 protocols). The data in Table 3 highlight a very high variability in almost all organs however, the organs at  
399 risk deserve a special focus.

400 For standard RIT treatments the major concern is the red marrow irradiation. In contrast, the major organs  
401 at risk for HD-RIT are the liver, the kidneys and the lungs depending on the radiopharmaceutical adopted.  
402 The corresponding variability factors for each organ among all authors are 0.5-2.1 for the liver, 0.6-1.64 for  
403 kidneys and 0.5-1.6 for the lungs.

404 Concerning the red marrow, Figure 2 shows the absorbed dose per unit of activity (Gy/GBq, range) for the  
405 most representative studies exploring different dosimetric approaches. The absorbed doses for Zevalin at  
406 standard and high activities are comparable, being based on the blood method. It was also shown that, for  
407 the <sup>90</sup>Y-epratuzumab-tetraxetan, the imaging method provides higher dose estimates than the blood  
408 method in the same patients. The study by Sgurous et al.<sup>73</sup> highlights the variations of dose estimations  
409 depending on the bone region used to extrapolate imaging data. All these studies show a quite relevant  
410 inter-patient variability. Although the most appropriate approach for red marrow dosimetry has not been  
411 established yet, there is some evidence showing that dosimetry obtained with the imaging method could  
412 better predict the toxicity data of standard RIT<sup>68</sup>. We should point out that, in the majority of the studies,  
413 the dosimetry data reported are based on 2D images, whose pitfalls are well known. The recent  
414 developments of equipment technology and computational models for dosimetry will certainly provide  
415 more accurate results than in the past. Hybrid approaches combining 2D and 3D imaging of activity  
416 distribution in organs at risk, adopted by some authors<sup>37,55,82</sup> are highly recommended. In case of <sup>131</sup>I-  
417 labelled radiopharmaceuticals, the use of the positron-emitting <sup>124</sup>I as a surrogate radioisotope for  
418 dosimetry would be desirable, although the costs and the availability are still demanding.

419 A further issue that deserves attention in the myeloblastic RIT is the appropriate timing for SCT. In fact, to  
420 be on the safe side for a successful engraftment, the radiation dose to the reinfused stem cells should be as  
421 low as possible. Different authors provided several empirical dose constraints for the proper time of SCT.

422 In particular, an absorbed dose  $\leq 50$  mGy ( $T_1$ ) to the Reinfused Stem Cells (RSC) or a dose rate  $\leq 10$  mGy/h to  
423 the red marrow ( $T_2$ )<sup>37</sup> were proposed. The criteria are depicted in Figure 3 based on the blood curve of a  
424 representative patient treated with HD-RIT <sup>90</sup>Y Zevalin<sup>56</sup>. For the first constraint, some Authors<sup>56</sup> assumed  
425 that RSC receive the same irradiation of the red marrow from the time of SCT to infinity (Figure 3c, pink  
426 triangle). However, considering that the RSC circulate in the blood pool for a certain time ( $\Delta$ ) before homing  
427 in the bone marrow, a potentially more accurate model should consider two different sources of irradiation  
428 in two time intervals: the first source of irradiation during the  $\Delta$  time would be the blood, the second being  
429 the red marrow up to infinity (Figure 3d).

430 Finally, we would like to emphasise that, besides any possible improvements of dosimetry accuracy and  
431 standardization, the absorbed doses are just one of the multiple parameters needed to predict the effects  
432 of therapy in term of both toxicity and efficacy. It is well known that, in radiation oncology, the clinical  
433 outcomes depend not only on the adsorbed dose but also on the tumour biology and on patient conditions.  
434 Today, novel molecular and genetic tests are available and may guide the choice of the most appropriate  
435 drug or immunotherapy. Currently available molecular and genetic biomarkers, along with personalised  
436 dosimetry, may enable to select the best candidates for HD-RIT. The final goal of precision nuclear  
437 oncology is to minimize acute and late toxicity whilst preserving efficacy.

438

439 **Conflict of Interest**

440 The authors declare no conflict of interest with regard to this paper.

441

## 442 **References**

- 443 1. Swerdlow SH, Campo E, Harris NL, et al: WHO Classification of Tumours of Haematopoietic and  
444 Lymphoid Tissues (ed 4 revised). Lyon, France, IARC, 2017
- 445 2. Yung L, Linch D: Hodgkin's lymphoma. *Lancet* 361:943-951, 2003
- 446 3. Shankland KR, Armitage JO, Hancock BW: Non-Hodgkin lymphoma. *Lancet* 380:848-857, 2012
- 447 4. Flinn IW, van der Jagt R, Kahl B, et al: First-Line Treatment of Patients With Indolent Non-Hodgkin  
448 Lymphoma or Mantle-Cell Lymphoma With Bendamustine Plus Rituximab Versus R-CHOP or R-CVP:  
449 Results of the BRIGHT 5-Year Follow-Up Study. *J Clin Oncol* 37:984-991, 2019
- 450 5. Witzig TE, Gordon LI, Cabanillas F, et al: Randomized controlled trial of yttrium-90-labeled ibritumomab  
451 tiuxetan radioimmunotherapy versus rituximab immunotherapy for patients with relapsed or refractory  
452 low-grade, follicular, or transformed B-cell non-Hodgkin's lymphoma. *J Clin Oncol* 20:2453-2463, 2002
- 453 6. Witzig TE, Flinn IW, Gordon LI, et al: Treatment with ibritumomab tiuxetan radioimmunotherapy in  
454 patients with rituximab-refractory follicular non-Hodgkin's lymphoma. *J Clin Oncol* 20:3262-3269, 2002
- 455 7. Fisher RI, Kaminski MS, Wahl RL, et al: Tositumomab and iodine-131 tositumomab produces durable  
456 complete remissions in a subset of heavily pretreated patients with low-grade and transformed non-  
457 Hodgkin's lymphomas. *J Clin Oncol* 23:7565-7573, 2005
- 458 8. Antonescu C, Bischof Delaloye A, Kosinski M, et al: Repeated injections of <sup>131</sup>I-rituximab show patient-  
459 specific stable biodistribution and tissue kinetics. *Eur J Nucl Med Mol Imaging* 32:943-951, 2005
- 460 9. Ilidge TM, Bayne M, Brown NS, et al: Phase 1/2 study of fractionated (131)I-rituximab in low-grade B-  
461 cell lymphoma: the effect of prior rituximab dosing and tumor burden on subsequent  
462 radioimmunotherapy. *Blood* 113:1412-1421, 2009
- 463 10. Leahy MF, Turner JH: Radioimmunotherapy of relapsed indolent non-Hodgkin lymphoma with <sup>131</sup>I-  
464 rituximab in routine clinical practice: 10-year single-institution experience of 142 consecutive  
465 patients. *Blood* 117:45-52, 2011



- 466 11. Scholz CW, Pinto A, Linkesch W, et al: (90)Yttrium-ibritumomab-tiuxetan as first-line treatment for  
467 follicular lymphoma: 30 months of follow-up data from an international multicenter phase II clinical  
468 trial. *J Clin Oncol* 31:308-313, 2013
- 469 12. Kaminski MS, Tuck M, Estes J, et al: <sup>131</sup>I-tositumomab therapy as initial treatment for follicular  
470 lymphoma. *N Engl J Med* 352:441-449, 2005
- 471 13. McQuillan AD, Macdonald WB, Turner JH: Phase II study of first-line (131)I-rituximab  
472 radioimmunotherapy in follicular non-Hodgkin lymphoma and prognostic (18)F-fluorodeoxyglucose  
473 positron emission tomography. *Leuk Lymphoma* 56:1271-1277, 2015
- 474 14. Jacene HA, Filice R, Kasecamp W: Comparison of <sup>90</sup>Y-ibritumomab tiuxetan and 131I-tositumomab in  
475 clinical practice. *J Nucl Med* 48:1767-1776, 2007
- 476 15. Cicone F, Russo E, Carpaneto A, et al: Follicular lymphoma at relapse after rituximab containing  
477 regimens: comparison of time to event intervals prior to and after 90 Y-ibritumomab-tiuxetan. *Hematol*  
478 *Oncol* 29:131-138, 2011
- 479 16. Morschhauser F, Radford J, Van Hoof A, et al: Phase III trial of consolidation therapy with yttrium-90-  
480 ibritumomab tiuxetan compared with no additional therapy after first remission in advanced follicular  
481 lymphoma. *J Clin Oncol* 26:5156-5164, 2008
- 482 17. Morschhauser F, Radford J, Van Hoof A, et al: 90Yttrium-ibritumomab tiuxetan consolidation of first  
483 remission in advanced-stage follicular non-Hodgkin lymphoma: updated results after a median follow-  
484 up of 7.3 years from the International, Randomized, Phase III First-Line Indolent trial. *J Clin Oncol*  
485 31:1977-1983, 2013
- 486 18. Karmali R, Larson ML, Shammo JM, et al: Phase 2 study of CHOP-R-14 followed by 90Y-ibritumomab  
487 tiuxetan in patients with previously untreated diffuse large B-cell lymphoma. *Mol Clin Oncol* 6:627-633,  
488 2017
- 489 19. Morschhauser F, Illidge T, Huglo D, et al: Efficacy and safety of yttrium-90 ibritumomab tiuxetan in  
490 patients with relapsed or refractory diffuse large B-cell lymphoma not appropriate for autologous stem-  
491 cell transplantation. *Blood* 110:54-8, 2007

- 492 20. Eskian M, Khorasanizadeh M, Isidori A, et al: Radioimmunotherapy-based conditioning regimen prior to  
493 autologous stem cell transplantation in non-Hodgkin lymphoma. *Int J Hematol Oncol* 7:IJH01, 2018
- 494 21. Krishnan A, Nademanee A, Fung HC, et al: Phase II trial of a transplantation regimen of yttrium-90  
495 ibritumomab tiuxetan and high-dose chemotherapy in patients with non-Hodgkin's lymphoma. *J Clin*  
496 *Oncol* 26:90-95, 2008
- 497 22. Kang BW, Kim WS, Kim C, et al: Yttrium-90-ibritumomab tiuxetan in combination with intravenous  
498 busulfan, cyclophosphamide, and etoposide followed by autologous stem cell transplantation in  
499 patients with relapsed or refractory B-cell non-Hodgkin's lymphoma. *Invest New Drugs* 28:516-522,  
500 2010
- 501 23. Khouri IF, Saliba RM, Erwin WD, et al: Nonmyeloablative allogeneic transplantation with or without  
502 90yttrium ibritumomab tiuxetan is potentially curative for relapsed follicular lymphoma: 12-year  
503 results. *Blood* 119:6373-6378, 2012
- 504 24. Shimoni A, Avivi I, Rowe JM, et al: A randomized study comparing yttrium-90 ibritumomab tiuxetan  
505 (Zevalin) and high-dose BEAM chemotherapy versus BEAM alone as the conditioning regimen before  
506 autologous stem cell transplantation in patients with aggressive lymphoma. *Cancer* 118:4706-4714,  
507 2012
- 508 25. Vose JM, Carter S, Burns LJ, et al: Phase III randomized study of rituximab/carmustine, etoposide,  
509 cytarabine, and melphalan (BEAM) compared with iodine-131 tositumomab/BEAM with autologous  
510 hematopoietic cell transplantation for relapsed diffuse large B-cell lymphoma: results from the BMT  
511 CTN 0401 trial. *J Clin Oncol* 31:1662-1668, 2013
- 512 26. Gopal AK, Rajendran JG, Petersdorf SH, et al: High-dose chemo-radioimmunotherapy with autologous  
513 stem cell support for relapsed mantle cell lymphoma. *Blood* 99:3158-3162, 2002
- 514 27. Gopal AK, Rajendran JG, Gooley TA, et al: High-dose [131I]tositumomab (anti-CD20)  
515 radioimmunotherapy and autologous hematopoietic stem-cell transplantation for adults > or = 60 years  
516 old with relapsed or refractory B-cell lymphoma. *J Clin Oncol* 25:1396-402, 2007

- 517 28. Gopal AK, Gooley TA, Rajendran JG, et al: Myeloablative I-131-tositumomab with escalating doses of  
518 fludarabine and autologous hematopoietic transplantation for adults age  $\geq$  60 years with B cell  
519 lymphoma. *Biol Blood Marrow Transplant* 20:770-775, 2014
- 520 29. Nademanee A, Forman S, Molina A, et al: A phase 1/2 trial of high-dose yttrium-90-ibritumomab  
521 tiuxetan in combination with high-dose etoposide and cyclophosphamide followed by autologous stem  
522 cell transplantation in patients with poor-risk or relapsed non-Hodgkin lymphoma. *Blood* 106:2896-  
523 2902, 2005
- 524 30. Winter JN, Inwards DJ, Spies S, et al: Yttrium-90 ibritumomab tiuxetan doses calculated to deliver up to  
525 15 Gy to critical organs may be safely combined with high-dose BEAM and autologous transplantation  
526 in relapsed or refractory B-cell non-Hodgkin's lymphoma. *J Clin Oncol* 27:1653-1659, 2009
- 527 31. Ferrucci PF, Vanazzi A, Grana CM, et al: High activity 90Y-ibritumomab tiuxetan (Zevalin) with  
528 peripheral blood progenitor cells support in patients with refractory/resistant B-cell non-Hodgkin  
529 lymphomas. *Br J Haematol* 139:590-599, 2007
- 530 32. Devizzi L, Guidetti A, Tarella C, et al: High-dose yttrium-90-ibritumomab tiuxetan with tandem stem-cell  
531 reinfusion: an outpatient preparative regimen for autologous hematopoietic cell transplantation. *J Clin*  
532 *Oncol* 26:5175-5182, 2008
- 533 33. Hohloch K, Sahlmann CO, Lakhani VJ, et al: Tandem high-dose therapy in relapsed and refractory B-cell  
534 lymphoma: results of a prospective phase II trial of myeloablative chemotherapy, followed by escalated  
535 radioimmunotherapy with (131)I-anti-CD20 antibody and stem cell rescue. *Ann Hematol* 90:1307-1315,  
536 2011
- 537 34. Bethge WA, von Harsdorf S, Bornhauser M, et al: Dose-escalated radioimmunotherapy as part of  
538 reduced intensity conditioning for allogeneic transplantation in patients with advanced high-grade non-  
539 Hodgkin lymphoma. *Bone Marrow Transplant* 47:1397-1402, 2012
- 540 35. Wagner JY, Schwarz K, Schreiber S, et al: Myeloablative anti-CD20 radioimmunotherapy +/- high-dose  
541 chemotherapy followed by autologous stem cell support for relapsed/refractory B-cell lymphoma  
542 results in excellent long-term survival. *Oncotarget* 4:899-910, 2013

- 543 36. Chow VA, Rajendran JG, Fisher DR, et al: A phase II trial evaluating the efficacy of high-dose  
544 Radioiodinated Tositumomab (Anti-CD20) antibody, etoposide and cyclophosphamide followed by  
545 autologous transplantation, for high-risk relapsed or refractory non-hodgkin lymphoma. *Am J Hematol*  
546 95:775-783, 2020
- 547 37. Wahl RL, Frey EC, Jacene HA, et al: Prospective SPECT-CT Organ Dosimetry-Driven Radiation-Absorbed  
548 Dose Escalation Using the In-111 (111In)/Yttrium 90 (90Y) Ibritumomab Tiuxetan (Zevalin®) Theranostic  
549 Pair in Patients with Lymphoma at Myeloablative Dose Levels. *Cancers (Basel)* 13:2828, 2021
- 550 38. Gisselbrecht C, Vose J, Nademanee A, et al: Radioimmunotherapy for stem cell transplantation in non-  
551 Hodgkin's lymphoma: in pursuit of a complete response. *Oncologist* 14 (suppl 2):41-51, 2009
- 552 39. Gopal AK, Gooley TA, Maloney DG, et al: High-dose radioimmunotherapy versus conventional high-dose  
553 therapy and autologous hematopoietic stem cell transplantation for relapsed follicular non-Hodgkin  
554 lymphoma: a multivariable cohort analysis. *Blood* 102:2351-2357, 2003
- 555 40. Krishnan A, Palmer JM, Tsai NC, et al: Matched-cohort analysis of autologous hematopoietic cell  
556 transplantation with radioimmunotherapy versus total body irradiation-based conditioning for poor-  
557 risk diffuse large cell lymphoma. *Biol Blood Marrow Transplant* 18:441-450, 2012
- 558 41. Pacilio M, Betti M, Cicone F, et al: A theoretical dose-escalation study based on biological effective dose  
559 in radioimmunotherapy with (90)Y-ibritumomab tiuxetan (Zevalin). *Eur J Nucl Med Mol Imaging* 37:862-  
560 873, 2010
- 561 42. Philip T, Guglielmi C, Hagenbeek A, et al: Autologous bone marrow transplantation as compared with  
562 salvage chemotherapy in relapses of chemotherapy-sensitive non-Hodgkin's lymphoma. *N Engl J Med*  
563 333:1540-1545, 1995
- 564 43. Epperla N, Hamadani M: Hematopoietic cell transplantation for diffuse large B-cell and follicular  
565 lymphoma: Current controversies and advances. *Hematol Oncol Stem Cell Ther.* 10:277-284, 2017
- 566 44. Colita A, Colita A, Bumbea H, et al. LEAM vs. BEAM vs. CLV Conditioning Regimen for Autologous Stem  
567 Cell Transplantation in Malignant Lymphomas. Retrospective Comparison of Toxicity and Efficacy on

- 568 222 Patients in the First 100 Days After Transplant, On Behalf of the Romanian Society for Bone  
569 Marrow Transplantation. *Front Oncol* 9:892, 2019
- 570 45. Sapelli J, Filho JS, Matias Vieira GM, et al: BuCyE can safely replace BEAM as a conditioning regimen for  
571 autologous stem cell transplantation in the treatment of refractory and relapsed lymphomas [published  
572 online ahead of print]. *Leuk Res* 110:106689, 2021
- 573 46. Bacher U, Klyuchnikov E, Le-Rademacher J, et al: Conditioning regimens for allotransplants for diffuse  
574 large B-cell lymphoma: myeloablative or reduced intensity?. *Blood* 120:4256-4262, 2012
- 575 47. Press OW, Eary JF, Appelbaum FR, et al: Radiolabeled-antibody therapy of B-cell lymphoma with  
576 autologous bone marrow support. *N Engl J Med* 329:1219-1224, 1993
- 577 48. Press OW, Eary JF, Appelbaum FR, et al: Phase II trial of 131I-B1 (anti-CD20) antibody therapy with  
578 autologous stem cell transplantation for relapsed B cell lymphomas. *Lancet* 346:336-340, 1995
- 579 49. Liu SY, Eary JF, Petersdorf SH, et al: Follow-up of relapsed B-cell lymphoma patients treated with iodine-  
580 131-labeled anti-CD20 antibody and autologous stem-cell rescue. *J Clin Oncol* 16:3270-3278, 1998
- 581 50. Press OW, Eary JF, Gooley T, et al: A phase I/II trial of iodine-131-tositumomab (anti-CD20), etoposide,  
582 cyclophosphamide, and autologous stem cell transplantation for relapsed B-cell lymphomas. *Blood*  
583 96:2934-42, 2000
- 584 51. Siegel JA, Thomas SR, Stubbs JB, et al: MIRD pamphlet no. 16: Techniques for quantitative  
585 radiopharmaceutical biodistribution data acquisition and analysis for use in human radiation dose  
586 estimates. *J Nucl Med* 40:37S-61S, 1999
- 587 52. Loevinger R, Budinger TF, Watson EE (eds): *MIRD Primer for absorbed dose calculations*. New York, NY,  
588 The Society of Nuclear Medicine, 1988
- 589 53. Assié K, Dieudonné A, Gardin I, et al: Comparison between 2D and 3D dosimetry protocols in 90Y-  
590 ibritumomab tiuxetan radioimmunotherapy of patients with non-Hodgkin's lymphoma. *Cancer Biother*  
591 *Radiopharm* 23:53-64, 2008

- 592 54. Sgouros G, Squeri S, Ballangrud AM, et al: Patient-specific, 3-dimensional dosimetry in non-Hodgkin's  
593 lymphoma patients treated with <sup>131</sup>I-anti-B1 antibody: assessment of tumor dose-response. *J Nucl*  
594 *Med* 44:260-268, 2003
- 595 55. Boucek JA, Turner JH: Validation of prospective whole-body bone marrow dosimetry by SPECT/CT  
596 multimodality imaging in (<sup>131</sup>I)-anti-CD20 rituximab radioimmunotherapy of non-Hodgkin's  
597 lymphoma. *Eur J Nucl Med Mol Imaging* 32:458-469, 2005
- 598 56. Cremonesi M, Ferrari M, Grana CM, et al: High-dose radioimmunotherapy with <sup>90</sup>Y-ibritumomab  
599 tiuxetan: comparative dosimetric study for tailored treatment [published correction appears in *J Nucl*  
600 *Med*. 2007 Dec;48(12):2027]. *J Nucl Med* 48:1871-1879, 2007
- 601 57. Chiesa C, Botta F, Coliva A, et al: Absorbed dose and biologically effective dose in patients with high-risk  
602 non-Hodgkin's lymphoma treated with high-activity myeloablative <sup>90</sup>Y-ibritumomab tiuxetan  
603 (Zevalin). *Eur J Nucl Med Mol Imaging* 36:1745-1757, 2009
- 604 58. Wiseman GA, Kornmehl E, Leigh B, et al: Radiation dosimetry results and safety correlations from <sup>90</sup>Y-  
605 ibritumomab tiuxetan radioimmunotherapy for relapsed or refractory non-Hodgkin's lymphoma:  
606 combined data from 4 clinical trials. *J Nucl Med* 44:465-74, 2003
- 607 59. Whal RL, Kroll S, Zasadny KR: Patient-specific whole-body dosimetry: principles and a simplified method  
608 for clinical implementation. *J Nucl Med* 39(8 Suppl):14S-20S, 1998
- 609 60. Whal RL, Zasadny KR, MacFarlane D, et al: Iodine-131 anti-B1 antibody for B-cell lymphoma: an update  
610 on the Michigan Phase I experience. *J Nucl Med* 39(8 Suppl):21S-27S, 1998
- 611 61. Press OW, Eary JF, Badger CC, et al: Treatment of refractory Non-Hodgkin's Lymphoma with  
612 radiolabeled MB-1 (Anti-CD37) antibody. *J Clin Onc* 8:1027-1038, 1989
- 613 62. Eary JF, Press OW, Badger CC, et al: Imaging and treatment of B-cell lymphoma. *J Nucl Med* 31:1257-  
614 1268, 1990
- 615 63. Bolch WE, Patton PW, Rajon DA, et al: Considerations of marrow cellularity in 3-dimensional dosimetric  
616 models of the trabecular skeleton. *J Nucl Med* 43:97-108, 2002

- 617 64. Sgouros G. Bone marrow dosimetry for radioimmunotherapy: theoretical considerations. *J Nucl Med*  
618 34:689-694, 1993
- 619 65. Shen S, DeNardo GL, Sgouros G, et al: Practical determination of patient-specific marrow dose using  
620 radioactivity concentration in blood and body. *J Nucl Med* 40:2102-2106, 1999
- 621 66. Siegel JA, Lee RE, Pawlyk DA, et al: Sacral scintigraphy for bone marrow dosimetry in  
622 radioimmunotherapy. *Int J Rad Appl Instrum B* 16:553-559, 1989
- 623 67. Buijs WC, Siegel JA, Boerman OC, et al: Absolute organ activity estimated by five different methods of  
624 background correction. *J Nucl Med* 39:2167-2172, 1998
- 625 68. Ferrer L, Kraeber-Bodéré F, Bodet-Milin C, et al: Three methods assessing red marrow dosimetry in  
626 lymphoma patients treated with radioimmunotherapy. *Cancer* 116 (suppl 4):1093-1100, 2010
- 627 69. Cristy M: Active bone marrow distribution as a function of age in humans. *Phys Med Biol* 26:389-400,  
628 1981
- 629 70. Vande Berg BC, Lecouvet FE, Moysan P, et al: MR assessment of red marrow distribution and  
630 composition in the proximal femur: correlation with clinical and laboratory parameters. *Skeletal Radiol*  
631 26:589-596, 1997
- 632 71. Richardson ML, Patten RM: Age-related changes in marrow distribution in the shoulder: MR imaging  
633 findings. *Radiology* 192:209-215, 1994
- 634 72. Kim SC, Krynycky BR, Machac J, et al: Patterns of red marrow in the adult femur. *Clin Nucl Med* 31:739-  
635 741, 2006
- 636 73. Sgouros G, Jureidini IM, Scott AM, et al: Bone marrow dosimetry: regional variability of marrow-  
637 localizing antibody. *J Nucl Med* 37:695-698, 1996
- 638 74. Stabin MG, Eckerman KF, Bolch WE, et al: Evolution and status of bone and marrow dose models.  
639 *Cancer Biother Radiopharm* 17:427-433, 2002
- 640 75. Spiers FW (ed): Beta dosimetry in trabecular bone in *Delayed Effects of Bone-Seeking Radionuclides*,  
641 edited by C.W. Mays Univ of Utah Press, Salt Lake City, UT, p. pp 95-108, Dec. 1969, [Online]. Available:  
642 <https://www.osti.gov/biblio/4746249>

643 76. Spiers FW, Whitwell JR, Beddoe AH: Calculated dose factors for the radiosensitive tissues in bone  
644 irradiated by surface-deposited radionuclides. *Phys Med Biol* 23:481-494, 1978

645 77. Cristy M, Eckerman KF (eds): Specific Absorbed Fractions of Energy at Various Ages from Internal  
646 Photons Sources. New York, NY, The Society of Nuclear Medicine, 1987

647 78. Bouchet LG, Bolch WE, Howell RW, et al: S values for radionuclides localized within the skeleton. *J Nucl*  
648 *Med* 41:189-212, 2000

649 79. Jokisch DW, Patton PW, Inglis BA, et al: NMR microscopy of trabecular bone and its role in skeletal  
650 dosimetry. *Health Phys* 75:584-596, 1998

651 80. Jokisch DW, Patton PW, Rajon DA, et al: Chord distributions across 3D digital images of a human  
652 thoracic vertebra. *Med Phys* 28:1493-1504, 2001

653 81. Rajon DA, Jokisch DW, Patton PW, et al: Voxel size effects in three-dimensional nuclear magnetic  
654 resonance microscopy performed for trabecular bone dosimetry. *Med Phys* 27:2624-2635, 2000

655 82. Cicone F., D'Arienzo M., Carpaneto A. et al: Quantification of dose nonuniformities by voxel-based  
656 dosimetry in patients receiving 90Y-ibritumomab-tiuxetan. *Cancer Biother Radiopharm* 28:98-107, 2013

657 83. Michelsen K: Determination in inulin, albumin and erythrocyte spaces in the bone marrow of  
658 rabbits. *Acta Physiol Scand* 77:28-35, 1969

659 84. Bartl R, Frisch B, Burkhardt R (eds): Bone marrow biopsies revisited (ed 2). New York, NY, Karger, 1985

660 85. Brunning RD, Bloomfield CD, McKenna RW, et al: Bilateral trephine bone marrow biopsies in lymphoma  
661 and other neoplastic diseases. *Ann Intern Med* 82:365-366, 1975

662 86. Snyder WS, Ford MR, Wagner GG, et al (eds): MIRD Pamphlet #11: S, Absorbed Dose per Unit  
663 Cumulated Activity for Selected Radionuclides and Organs. New York, NY, The Society of Nuclear  
664 Medicine, 1975

665 87. Ganong WF (ed): Review of Medical Physiology (ed 12). Los Altos, CA, Lange Medical Publications, 1985

666 88. Stabin MG, Sparks RB, Crowe E: OLINDA/EXM: the second-generation personal computer software for  
667 internal dose assessment in nuclear medicine. *J Nucl Med* 46:1023-1027, 2005

668



- 669 89. Whitwell JR, Spiers FW: Calculated beta-ray dose factors for trabecular bone. *Phys Med Biol* 21:16-38,  
670 1976
- 671 90. Cassaday RD, Stevenson PA, Gooley TA, et al: High-dose CD20-targeted radioimmunotherapy-based  
672 autologous transplantation improves outcomes for persistent mantle cell lymphoma. *Br J Haematol*  
673 171:788-797, 2015
- 674 91. Kaminski MS, Zasadny KR, Francis IR, et al: Radioimmunotherapy of B-cell lymphoma with [131I]anti-B1  
675 (anti-CD20) antibody. *N Engl J Med* 329:459-465, 1993
- 676 92. Hattori N, Gopal AK, Shields AT, et al: 131I-tositumomab myeloablative radioimmunotherapy for non-  
677 Hodgkin's lymphoma: radiation dose to the testes. *Nucl Med Commun* 33:1225-1231, 2012
- 678 93. Delaloye AB, Antonescu C, Louton T, et al: Dosimetry of 90Y-ibritumomab tiuxetan as consolidation of  
679 first remission in advanced-stage follicular lymphoma: results from the international phase 3 first-line  
680 indolent trial. *J Nucl Med* 50:1837-1843, 2009
- 681

## 682 Appendix A

683

### 684 a. Bone marrow dosimetry without specific uptake

685 In their model, Sgouros et al.<sup>64</sup> assume a rapid equilibrium in both plasma and extracellular fluid and the  
686 absence of specific uptake, i.e the absence of binding between the administered antibodies and any  
687 component of the blood, marrow, or bone. As a consequence, an equilibrium of agents is rapidly achieved  
688 after injection. Under the assumption of non-specific uptake, Sgouros et al.<sup>64</sup> proposed two methodologies  
689 for red marrow dose estimation, based respectively on blood samples and red marrow biopsy.

690 The simplest method is the one based on the red marrow-to-blood concentration ratio. It relates the  
691 activity concentration in blood  $[A]_{BL}$  to the one in plasma  $[A]_P$  by the hematocrit ( $HCT$ ):

$$[A]_P = \frac{[A]_{BL}}{1 - HCT} \quad \text{Eq. 1}$$

692

693 Since the activity concentration in plasma is assumed equal to the one in the extracellular volume of the  
694 red marrow, the activity concentration in marrow is simply expressed as:

$$[A]_{RM} = \frac{[A]_P \cdot V_{RMECF}}{V_{RM}} \quad \text{Eq. 2}$$

695

696 where  $V_{RMECF}$  = red marrow extracellular fluid volume and  $V_{RM}$  = red marrow volume.

697 Thus the red marrow-to-blood activity concentration ratio ( $RMBLR$ ) is:

$$RMBLR = \frac{[A]_{RM}}{[A]_{BL}} = \frac{V_{RMECF}}{V_{RM}} \cdot \frac{1}{1 - HCT} = RMECF \cdot \frac{1}{1 - HCT} = \frac{0.19}{1 - HCT} \quad \text{Eq. 3}$$

698

699 where  $RMECF$  is the red marrow to extracellular fluid fraction<sup>83</sup>.

700 The second method proposed by Sgouros et al.<sup>64</sup> is based on the time-activity concentration curve  
701 extracted from bone marrow biopsy. This method is considered the gold standard but, while in the first  
702 case it is sufficient to take small amounts of blood, in this case it is necessary to sample the marrow to  
703 calculate the concentration of activity in the red marrow. The marrow biopsy is composed of a thickness of  
704 cortical bone at both ends and an internal region of trabecular bone. This latter part contains in its  
705 honeycomb structure red marrow, fat (yellow marrow) and blood. Therefore, when the marrow activity  
706 concentration is obtained from the complete biopsy, different correction factors taking into account the  
707 biopsy components have to be applied. In fact, under the assumption that radiolabeled antibodies do not  
708 bind to these components, the activity concentration in marrow may be underestimated if the marrow  
709 mass is overestimated.

710 If the cortical bone is present in the biopsy, the cortical bone correction factor ( $CBC$ ) can be expressed as:

$$CBC = \frac{[A]_{RM}}{[A]_{BIOPSY}} = \left[ 1 + \left( \frac{CBF}{1 - CBF} \right) \frac{\rho_{CB}}{\rho_{RM}} \right] \quad \text{Eq. 4}$$

711

712 where  $[A]_{BIOPSY}$  = activity concentration in red marrow,  $CBF$  = volumetric fraction of the cortical bone in  
 713 the biopsy,  $\rho_{CB}$  = cortical bone density and  $\rho_{RM}$  = red marrow density.  $CBC$  baseline value is 1.42 and it  
 714 ranges from 1.1 to 1.9 for  $CBF$  of 0.06-0.32<sup>84</sup>.

715 When the cortical bone portion is removed from the biopsy, the presence of trabecular bone should be  
 716 considered anyway. Similarly to the cortical bone, the trabecular bone conversion factor (TBC) can be  
 717 expressed as:

$$TBC = \frac{[A]_{RM}}{[A]_{BIOPSY}} = \left[ 1 + \left( \frac{TBF}{1 - TBF} \right) \frac{\rho_{TB}}{\rho_{RM}} \right] \quad \text{Eq. 5}$$

718

719 where  $TBF$  = trabecular bone volumetric fraction in the biopsy and  $\rho_{CB}$  = cortical bone density.  $TBC$  baseline  
 720 value is 1.66 and it ranges from 1.3 to 2.1 for  $TBF$  of 0.12-0.38<sup>84</sup>.

721 Given a completely bone-free biopsy, a certain component of the sample is composed by yellow marrow.  
 722 Therefore, a fatty tissue correction factor ( $FTC$ ) can be expressed as:

$$FTC = \frac{[A]_{RM}}{[A]_{BIOPSY}} = \left[ 1 + \left( \frac{FTF}{1 - FTF} \right) \frac{\rho_{FT}}{\rho_{RM}} \right] \quad \text{Eq. 6}$$

723

724 where  $FTF$  = yellow marrow volumetric fraction in the biopsy and  $\rho_{FT}$  = yellow marrow density.  $FTC$   
 725 baseline value is 1.37 and it ranges from 1.1 to 1.7 for  $FTF$  of 0.08-0<sup>84</sup>.

726 In case of a completely bone- and fat-free biopsy, only the blood contamination remains, which may lead to  
 727 an overestimation of the marrow activity concentration. In this case, the activity concentration in the red  
 728 marrow can be expressed as:

$$[A]_{RM} = [A]_{BIOPSY} \cdot \left[ 1 + \left( \frac{BLF}{1 - BLF} \right) \frac{\rho_{BL}}{\rho_{RM}} \right] - [A]_{BL} \cdot \left[ \frac{BLF}{1 - BLF} \cdot \frac{\rho_{BL}}{\rho_{RM}} \right] \quad \text{Eq. 7}$$

729

730 where  $BLF$  = blood volumetric fraction in the biopsy and  $\rho_{BL}$  = blood density.

731 This equation can be directly used to correct the biopsy activity concentration, as the blood concentration  
 732 in the sample can be easily obtained. The blood correction factor ( $BLC$ ) can be also expressed by  
 733 substituting  $[A]_{BL}$  from Eq. 3:

$$BLC = \frac{[A]_{RM}}{[A]_{BIOPSY}} = \left[ \frac{1 + \left( \frac{BLF}{1 - BLF} \right) \frac{\rho_{BL}}{\rho_{RM}}}{1 + \left( \frac{1 - HCT}{RMECFF} \cdot \frac{BLF}{1 - BLF} \right) \frac{\rho_{BL}}{\rho_{RM}}} \right]$$

Eq. 8

734 *BLC* baseline value is 0.85 and it ranges from 0.96 to 0.69 for *BLF* of 0.02-0.24<sup>84</sup>.

735 For an untreated biopsy sample, containing all the contamination components, the appropriate correction  
736 factor is the product of the correction factors for each biopsy component and it converts the activity  
737 concentration in the whole sample to the activity concentration in the red marrow component. For  
738 standard biopsy samples baseline values of the correction factors can be used.

739 The described methods are suitable not only for radiolabeled antibodies, but for any labeled agent that  
740 rapidly reaches an equilibrium within the extracellular fluid region of the red marrow and that does not  
741 bind to any marrow, blood or bone component.

742

## 743 **b. Bone marrow dosimetry with specific uptake**

744 The methods for calculating activity concentration in red marrow shown above were based on the  
745 assumption that radiolabeled agents did not bind to any component of bone, marrow, or blood. These  
746 methods can be justified when less than 25% of red marrow is involved in dose absorption, thus assuming  
747 negligible consequences in marrow toxicity. However, red marrow involvement is usually assessed by an  
748 iliac crest bone marrow biopsy, which is often associated with false-negative results<sup>85</sup>. To overcome this  
749 limitation, Ferrer et al.<sup>68</sup> evaluated three different red marrow dosimetric methods in B-cell NHL patients  
750 that received 2 co-administrations of <sup>90</sup>Y-labeled and <sup>111</sup>In-labeled antibodies. The methods investigated are  
751 one image-based method (M1) and two blood-based methods (M2, M3).

752 Based on the MIRD approach<sup>52</sup>, the mean absorbed dose to the red marrow is expressed as:

$$D_{RM} = \widetilde{A}_{RM} \cdot S_{RM \leftarrow RM} + \sum_h \widetilde{A}_h \cdot S_{RM \leftarrow h} + \widetilde{A}_{RB} \cdot S_{RM \leftarrow RB}$$

Eq. 10

753

754 where  $\widetilde{A}_{RM}$ ,  $\widetilde{A}_h$  and  $\widetilde{A}_{RB}$  are the accumulated activity in the red marrow, in the source organ *h* and in the  
755 remainder of the body, respectively. Similarly,  $S_{RM \leftarrow RM}$ ,  $S_{RM \leftarrow h}$  and  $S_{RM \leftarrow RB}$  are the S value for RM self-  
756 irradiation, the S value for irradiation from source organ *h* and from the remainder of the body,  
757 respectively<sup>86</sup>. In the two blood-based methods,  $\widetilde{A}_{RM}$  is calculated as:

758

$$\widetilde{A}_{RM} = RMBLR \cdot C_{BL} \cdot m_{RM} = RMECFF \cdot \frac{1}{1 - HCT} \cdot C_{BL} \cdot m_{RM}$$

Eq. 11

759

760 where  $m_{RM}$  is the red marrow mass (fixed at 1500 g<sup>86</sup>),  $RMECF$  is 0.19, according to the Sgouros results,  
761 leading to a  $RMBLR$  of 0.36 for a normal value of  $HCT$  (0.47 for standard man)<sup>87</sup>.

762 The M2 approach assumes  $RMBLR$  constant and equal to 0.36 for all patients, whereas in the M3 approach  
763  $RMBLR$  depends on the patient's  $HCT$ . The cumulated activity in blood,  $C_{BL}$ , is calculated from the blood  
764 time-activity curve.

765 The image-based M1 method is more complex, requiring several imaging sessions and image/data  
766 processing, but it allows considering individual differences in marrow mass and uptake. This method  
767 assumes that red marrow mass in L<sub>2</sub>-L<sub>4</sub> lumbar vertebrae is proportional to trabecular bone volume and red  
768 marrow mass in this region is 6.7% of the red marrow mass in the whole body<sup>88</sup>. Therefore, marrow mass  
769 considered in dose calculation is patient-specific and red marrow absorbed dose can be obtain as:

$$D_{RM} = \frac{\widetilde{A}_{L_2-L_4}}{0.067} \cdot S_{RM \leftarrow RM} \cdot \frac{V_{trab L_2-L_4}^{refman}}{V_{trab L_2-L_4}^{patient}}$$

Eq. 12

770 with S values from the MIRD Pamphlet 11,  $V_{trab L_2-L_4}^{refman}$  = trabecular bone volume of the Reference Man,  
771  $V_{trab L_2-L_4}^{patient}$  = patient trabecular bone volume (from CT) and  $\widetilde{A}_{L_2-L_4}$  = cumulated activity in red marrow in L<sub>2</sub>-  
772 L<sub>4</sub> lumbar vertebrae (calculated from the time-activity curve of these regions).

773 Combining red marrow doses with platlet and leukocyte toxicity, M1 is the method which provides the best  
774 absorbed dose-effect relation as compared with the blood-based methods. Methods M2 shows almost the  
775 same results than M3 in red marrow doses, but both seem to have no correlation at all with the observed  
776 toxicity. Therefore, even for patients with low bone marrow involvement (less than 25%) it is important to  
777 consider bone marrow uptake of the radiolabeled agents.

### 778 c. Regional variability of marrow-localizing agents

779 The above described methods are based on the assumption of red marrow homogeneous distribution. The  
780 data form a single region (either blood sample, single biopsy or specific bone region such as L2-L4) are used  
781 for whole red marrow dose estimation. In fact, a linear factor is used for scaling the dose estimated for a  
782 single data to the whole red marrow. However, large inter- and intra-patients differences in red marrow  
783 distribution may occur that largely impact dosimetric evaluation<sup>69,70,71,72</sup>. Sgouros et al.<sup>73</sup> demonstrated the  
784 importance of this variability. They studied three different methods to calculate the mean absorbed dose to  
785 the whole red marrow in 10 patients infused with <sup>131</sup>I radiolabeled antibodies, in order to evaluate the  
786 dosimetric impact of a non uniform distribution of the activity concentration in the marrow. After the  
787 injection of the antibodies, patients were scanned front and back with a gamma camera on the day of the  
788 injection and daily for the next 3 days. Images were corrected for the background, the attenuation and the  
789 geometric mean was used. Some regions were selected as regions of interest: liver, spleen, thyroid, all  
790 femur's head and necks, all humerus' head and necks, two lumbar vertebrae (L3 and L4) and finally the  
791 whole body. Selected marrow regions (femur's head and necks, humerus' head and necks, L3-L4 lumbar  
792 vertebrae) had the minimal overlaying of tissues. Blood samples were also acquired post injection. No  
793 statistically significant difference of half-lives was found among femoral (mean ± standard deviation = 50 ±  
794 20 hr), lumbar (50 ± 20 hr), humeral (50 ± 10 hr) regions, or blood samples (37 ± 9 hr) and whole body (50 ±

795 10 hr). However, absorbed dose differences were observed. For each region, the cumulated activity was  
796 calculated from the time-activity curve fitted with a single exponential curve. The absorbed dose to each  
797 red marrow region (rg) was calculated using the equation:

$$D_{rg} = \widetilde{A}_{rg} \cdot S_{rg \leftarrow rg} + \widetilde{A}_{wb} \cdot S_{rm \leftarrow wb} \quad \text{Eq. 13}$$

798 where:

799 -  $\widetilde{A}_{rg}$ ,  $\widetilde{A}_{wb}$  = cumulated activity in the red marrow region rg and in the whole body respectively;

800 -  $S_{rg \leftarrow rg}$  = S-factor for the self-irradiation of the specific red marrow region rg;

801 -  $S_{rm \leftarrow wb}$  = S-factor for the cross irradiation of the whole body to red marrow.

802 The S-factors of corresponding body region (*i.e.* legs, arms and spine) were rescaled from the MIRD  
803 Pamphlet 11 based on the mass of the single region considered (*i.e.* femoral, humeral and L3-L4 regions  
804 respectively). This results in a large difference of mean absorbed dose among regions:  $0.7 \pm 0.3$  mGy/MBq  
805 for the femoral region  $1.0 \pm 0.3$  mGy/MBq for the humeral region and  $2.2 \pm 0.5$  mGy/MBq for L3-L4.  
806 Therefore, the difference in both mass and S-values strongly impact the absorbed dose estimation beyond  
807 the similarities in half-lives.

808 Then the total dose to the whole red marrow was calculated using 3 different approaches:

- 809 a) Assuming the cumulated activity concentration in the femur as representative of the whole marrow  
810 (with S-factors from MIRD Pamphlet 11);  
811 b) Using a volume-weighted average of the local marrow cumulated activity concentration in all  
812 considered regions (with S-factors from MIRD Pamphlet 11);  
813 c) Using a weighted average absorbed dose of all considered regions (with regional S-factors from  
814 MIRDOSE3).

815 This results in a mean absorbed dose to the red marrow equal to  $1.7 \pm 0.8$  mGy/MBq,  $2.2 \pm 0.6$  mGy/MBq  
816 and  $1.4 \pm 0.3$  mGy/MBq with the three proposed methods respectively. The impact of lower activity  
817 concentration measured in the femoral region is evident comparing the results of Method a to Method b.  
818 Moreover, the result of Method c, compared to one of Method b, reflects the lower (regional) S-factors  
819 used in MIRDOSE3 for the marrow self-irradiation than the values implemented in MIRD Pamphlet 11.  
820 Large differences were observed among patients in all considered regions and results showed a large inter-  
821 and intra-patient variability. Moreover red marrow depletion is not uncommon during radiotherapy  
822 treatments so the dosimetry based on a single-site activity concentration measure may not properly  
823 estimate possible marrow toxicity in any patient. Since patients were affected by leukemia, such variability  
824 could be caused by the antigen-positive cell distribution (which is also patient-specific).

825

## 826 **d. Evolution of bone and red marrow dose models (S-values)**

827 In the last decades several approaches for dosimetric evaluation in radioimmunotherapy have been  
828 proposed and they differ for both mathematical model and phantom used to mimic the human body. As  
829 for all other organs, the red marrow conversion factors between disintegrations in some regions to

830 absorbed dose in a target region were influenced by the evolution of phantom definition and calculation  
831 model<sup>74</sup>.

832 A first evaluation of dose conversion factors (DFs) for marrow irradiation by beta-emitting radionuclides  
833 within the trabecular bone was done by Spiers et al. from the early 1960s through the late 1970s<sup>75,76,89</sup>. In  
834 this model, electrons lose energy under the assumption of the continuous slowing down approximation  
835 (CSDA), irradiating both the trabecula of origin and the surrounding trabeculae and cavities containing red  
836 marrow. The electron's path through these regions was estimated by statistical evaluations of the chord  
837 length distribution in experiments with trabecular bone samples. Therefore average energy deposition in  
838 marrow from beta-emitters in bone was calculated.

839 Snyder et al. extended Spiers' work deriving the absorbed fractions for this case and other cases such as  
840 the bone marrow self irradiation with Monte Carlo codes. These results were used by the MIRD Committee  
841 to build S-values in MIRD Pamphlet No. 11<sup>86</sup>. In this Pamphlet the photon absorbed fractions for bone-  
842 marrow irradiation were conservatively high for low energy photons. Cristy and Eckerman<sup>77</sup> solved this  
843 problem, improving the low energy photon calculations. In particular, they independently modelled the  
844 energy deposition by secondary electrons derived from photon interactions in bone, but still relying on the  
845 chord-length distribution of Spiers. Therefore they obtained the electron absorbed fractions for different  
846 bone groups and a wide range of energies. The Cristy/Eckerman phantom model allowed to directly  
847 calculate the absorbed dose to the marrow from electrons originating in the marrow regions. Moreover,  
848 different Cristy/Eckerman phantoms were developed for both male and female and for different ages from  
849 newborns to adult age. The Cristy/Eckerman model is implemented in MIRDOSE3, which provides doses for  
850 adult males, adult females and children, as well as regional and skeletal average dose conversion factors.  
851 MIRDOSE2 software implemented the ICRP 30 phantom, mainly used for radiation protection purposes on  
852 workers because it was intended to be conservative. For this reason, it is not useful in predicting doses to  
853 red marrow in the context of patient specific dosimetry.

854 Bouchet et al.<sup>78</sup> developed a model still based on the Spiers' chord-length distribution, but employing a 3D  
855 electron transport algorithm, in both trabecular and cortical bone, using EGS4 Monte Carlo transport code.  
856 They calculated new absorbed fractions to generate new S-values for 22 skeletal sites.

857 The MIRD 11 model provides only the average marrow S-value for self-irradiation for reference adult male.  
858 The Eckerman et al. and Bouchet et al. models also provide local values for a specific region of the skeleton.  
859 Both models are accurate in electron transport algorithms and give good detailed internal doses. However  
860 they differ in three main points:

- 861 a) Eckerman supposed that absorbed fractions for red marrow self-irradiation should be obtained by  
862 multiplying absorbed fractions for marrow space self-irradiation by marrow cellularity, while  
863 Bouchet assumed that they were numerically equal without this multiplication. Eckerman values  
864 are 50% lower than those calculated by Bouchet.
- 865 b) Eckerman implemented 2D planar sources at the interface between the trabecular and marrow  
866 cavities, assuming the 10 $\mu$ m layer of soft tissue (endosteum) on the bone interface as a part of the  
867 red marrow. On the contrary, Bouchet assumed a source distribution throughout this layer of soft  
868 tissue. Dose factors in the Bouchet model for bone surface sources were about 1.5-2 times higher  
869 than the Eckerman ones.
- 870 c) Electron passing through the 10 $\mu$ m layer of soft tissue had a uniform distribution of angles in the  
871 Eckerman model, while in the Bouchet model had a uniform distribution of the cosine angle. Dose

872 factors in the Bouchet model for bone surface as a target were about 2 times higher than the  
873 Eckerman results.

874 The University of Florida conducted studies on these two models using 3D transport techniques in  
875 trabecular bone, based on NMR microscopy images which allowed to differentiate the active marrow (red)  
876 from the inactive marrow (yellow) regions<sup>79,80,81</sup>. They showed that none of the models accurately predicts  
877 the absorbed fraction for red marrow self-irradiation in the energy range from 20keV to 200keV. The  
878 Eckerman model underestimates the fraction at energies below 200keV, while the Bouchet model  
879 overestimates these values at energies higher than 20keV. Therefore they proposed an adjusted model  
880 where the Bouchet results are applied at low energies (below 10keV), while Eckerman results are applied at  
881 energies above 100keV. Intermediate values are assumed in the energy range 10-100keV.



## Acronyms

A:	Attenuation
ASCT:	Autologous Stem Cell Transplantation
B:	Background
Bexxar®	<sup>131</sup> I-tositumomab
BEAM:	carbustine, etoposide, cytarabine and melphalan chemotherapy.
DLBCL:	Diffuse large B-cell lymphoma
DLT:	Dose Limiting Toxicity
FL:	Follicular lymphoma
GM:	Geometric mean
HCT:	Hematocrit
HD-RIT:	High Dose Radioimmunotherapy
HL:	Hodgkin's lymphomas
MCL:	Mantle Cell Lymphomas
MTD:	Maximum Tolerated Dose
n.a.:	not available
NHL:	Non-Hodgkin Lymphoma
OM:	Organ masses
RIT:	Radioimmunotherapy
RM:	Red Marrow
RSC:	Reinfused Stem Cells
S:	Scatter
SPECT:	Single-Photon Emission Computerized Tomography
TANDEM:	Protocol combining HD-chemotherapy + ASCT and HD-RIT + ASCT
TB:	Total Body
TBI:	Total Body Irradiation
Zevalin®	<sup>90</sup> Y-ibritumomab-tiuxetan

## Figures' captions

**Figure 1.** Absorbed doses (median values, Gy) to normal organs for a)  $^{131}\text{I}$ -MoAbs+ASCT and b)  $^{90}\text{Y}$ -MoAbs+ASCT, reported by different authors. TB stands for Total Body.

**Figure 2.** Absorbed per unit activity (Gy/GBq) to the RM (median values and ranges of variability) for different therapy and dosimetry approaches (b=blood model; i L = imaging, lumbar vertebrae; i H = imaging, humerus; i F= imaging, femoral head). The absorbed doses for Zevalin at standard and high activities are comparable, despite quite high variability. The  $^{90}\text{Y}$ -epratuzumab tetraxetan (Ferrer et al. <sup>68</sup>) shows much higher evaluation when derived for imaging as compared to the blood method in the same patients. The values for by Kaminski et al. <sup>91</sup> For  $^{131}\text{I}$ -Bexxar have been extrapolated from the absorbed doses provided for blood, using the blood model, with  $D_{\text{RM}} = 0,36 \times D_{\text{blood}}$ . The study by Sgourous et al. <sup>73</sup> refers to a different antibody but highlights the regional variability of the RM doses from imaging of I-131- MoAb.

**Figure 3.** Time-activity curves for blood and RM to estimate the absorbed dose to the RSC.

The black line is the Time Activity Curve for the blood with the experimental time points of blood sampling (black crosses). The red line is Time Activity Curve for the RM, extrapolated from the blood model or evaluated from imaging. The %IA is in logarithmic scale. In this example the  $T_{1/2 \text{ eff}} = 32 \text{ h}$

Figure 3.a: The dashed area in black is the time integrated activity (TIA) for the blood allowing to evaluate the absorbed dose to the blood.

Figure 3.b: The dashed area in red is the TIA for the RM.

Figure 3.c: The larger pink triangle represents the TIA to the RSC under the hypothesis RSC receives the same irradiation as RM from the time ASCT to infinity.  $T_1$  is the time that guarantees a constraint of 50 mGy to RM.  $T_2$  is time that guarantees a constraint of dose rate to RM  $\leq 10$  mGy/h (Whal et al.<sup>37</sup>).

Figure 3.d: The trapezoid grey area represents the TIA to RSC due to the irradiation from the time of ASCT until the RSC homing. The smaller pink triangle represents TIA of the RSC after the homing.  $\Delta$  represents the time needed for SCT homing. The total irradiation is related to the sum of grey and pink areas.

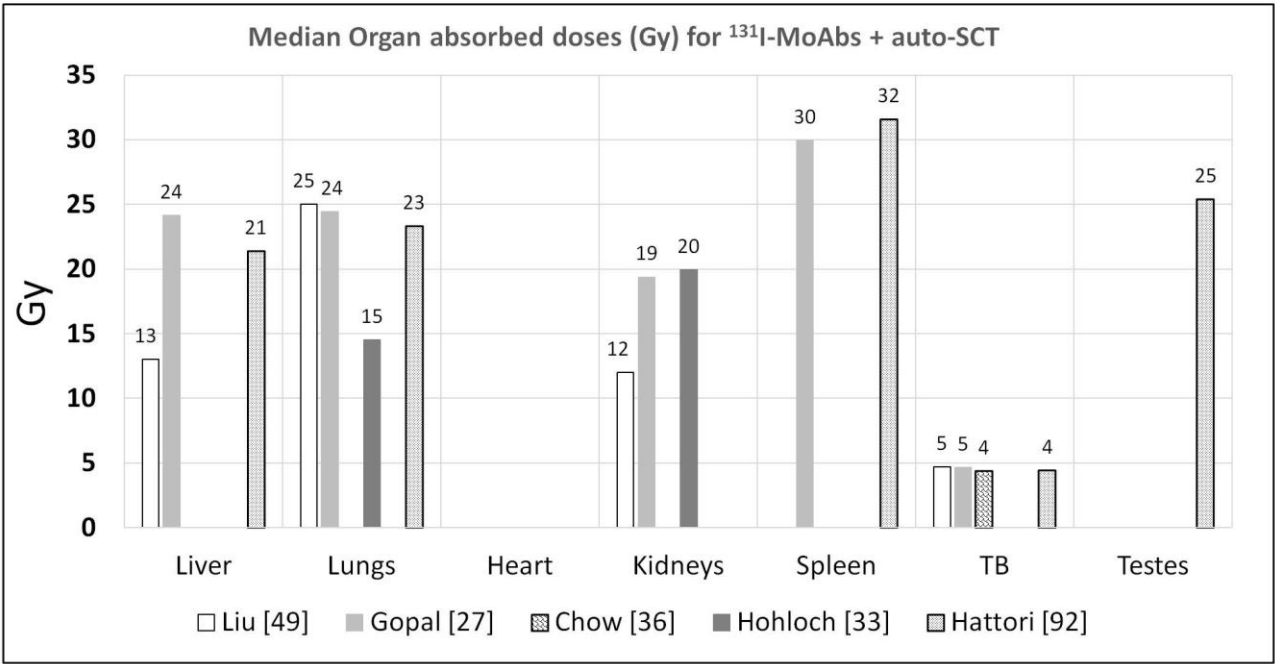
### **Tables' captions**

**Table 1.** Summary of the main clinical protocol used by different authors for NHL HD RIT.

**Table 2.** Summary of the previsional dosimetry methods used by different authors for NHL RIT. The first four studies concern standard approaches with dosimetry for RM . The other studies refer to high activity treatments associated with ASCT.

**Table 3.** Ranges of variability factors related to the absorbed doses to normal organs, normalised to the median absorbed dose values.

**a**



**b**

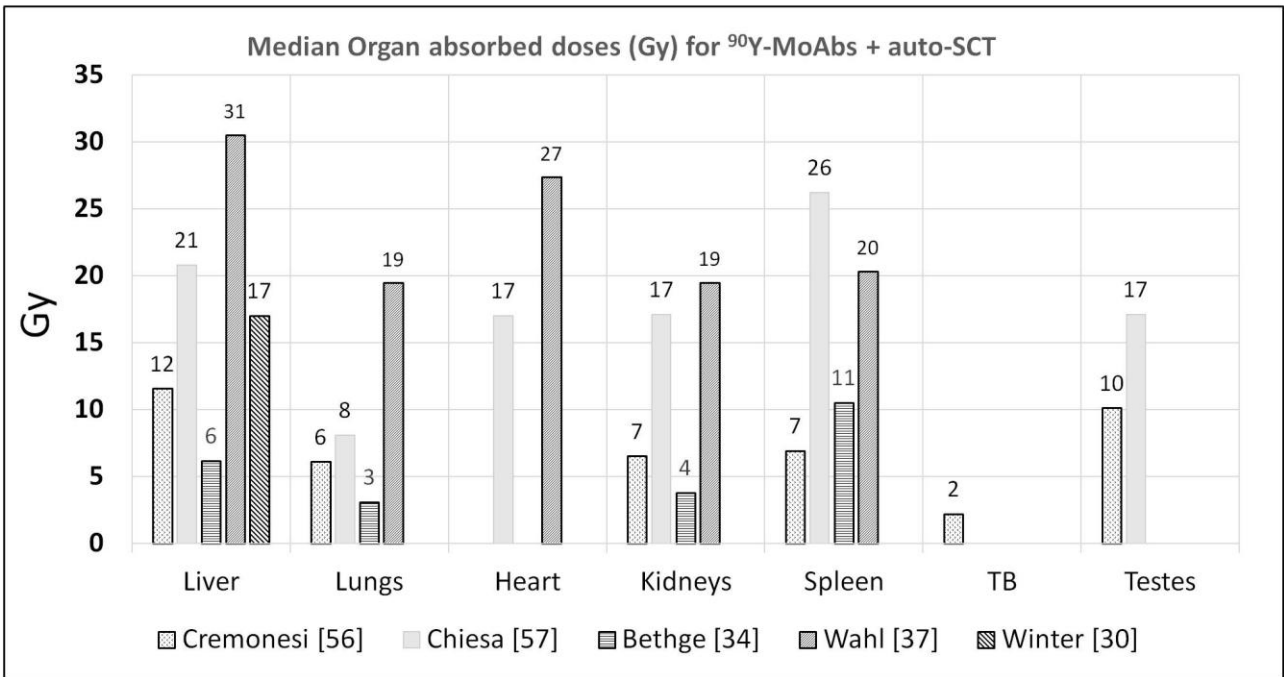


**Fig. 1**

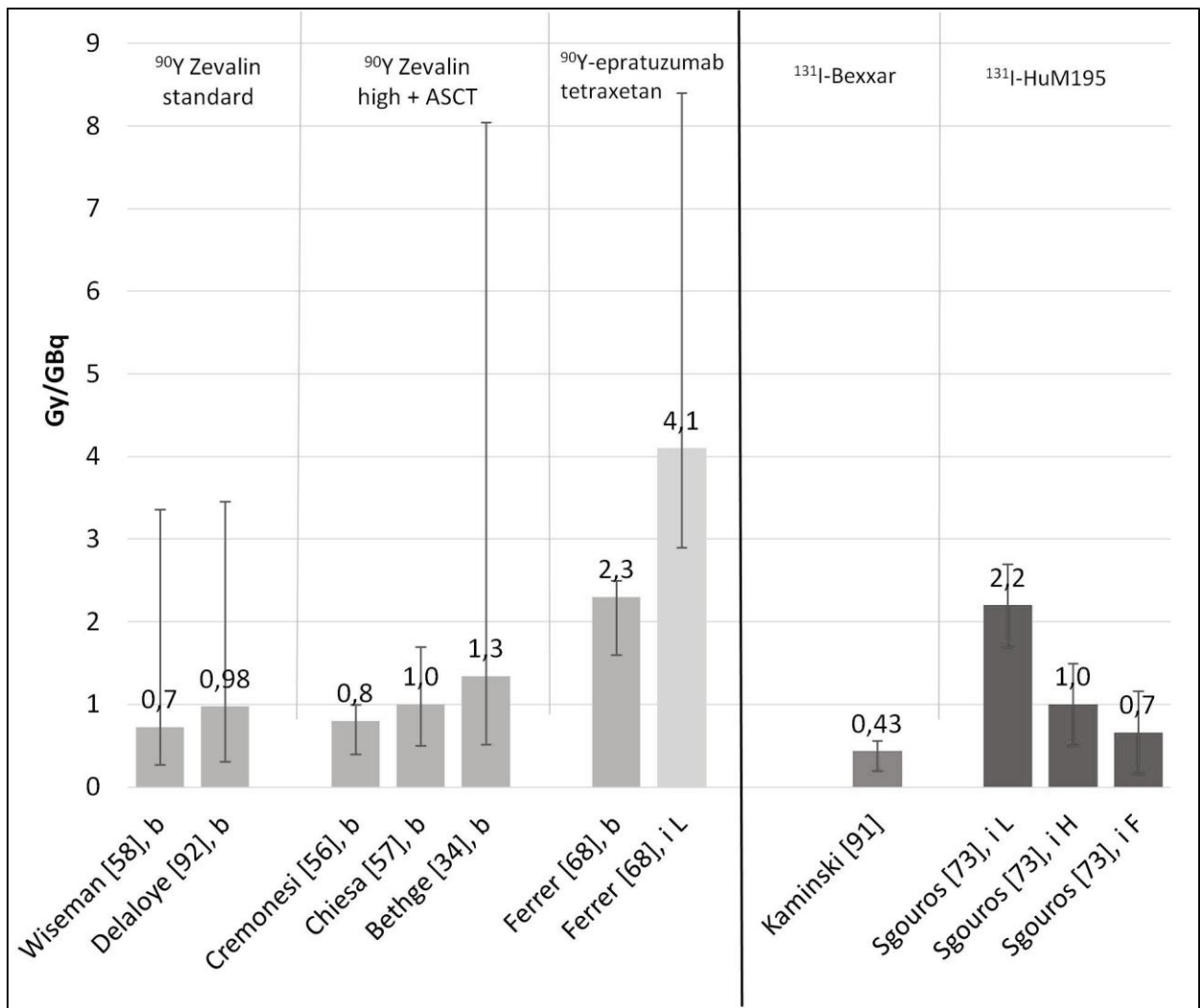
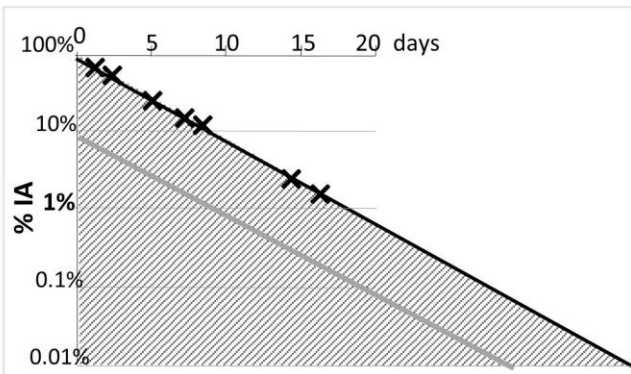
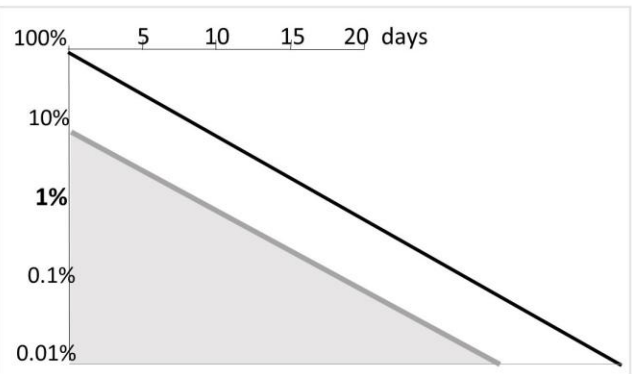


Fig. 2

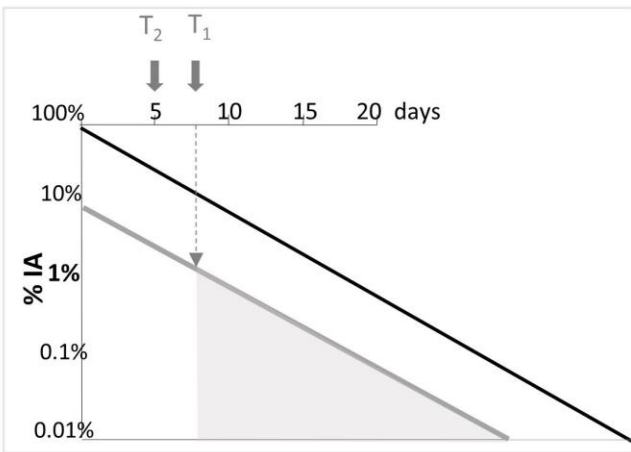
a



b



c



d

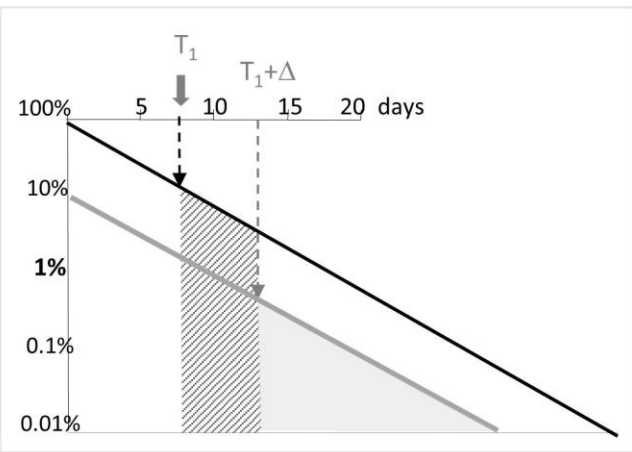


Fig. 3

Table 1. Summary of the main clinical protocol used by different authors for NHL HD RIT.									
AUTHOR [ref]	Radiopharmaceutical	Cold MoAb preloading	Type of disease	No patients	Activity administered	ASCT time	Dose constrains	Major OAR	Chemotherapy
<b>Y-90-MoAbs</b>									
Nademane [29]	Zevalin	rituximab 250 mg/m <sup>2</sup>	follicular lymphoma (n = 12), diffuse large B-cell (n = 14), and mantle cell (n = 5)	29	1.3 -3.9 GBq	radiation dose to RSC < 50 mGy	10 Gy to highest normal organ	Liver	high-doseetoposide (1P-16) 40 to 60 mg/kg (day -4) and cyclophosphamide 100 mg/kg (day -3)
Ferrucci[31]	Zevalin	rituximab 250 mg/m <sup>2</sup>	resistant/refractory B-cell NHL	13	Activity escalation: group I: 29.6 MBq/kg 4 patients group II: 44.4 MBq/kg for 4 patients group III: 55.5 MBq/kg 14 patients	ASCT @ 13 d p.L***	< 20 Gy to uninvolved organs (except RM) Dose to reinfused stem cells < 50 mGy	Liver	none
Devizzi [32]	Zevalin	rituximab 250 mg/m <sup>2</sup>	relapsed/refractory or de-novo high-risk NHL	30	Activity escalation: 30 MBq/kg 15 patients 45 MBq/kg for 17 patients	ASCT @ 7 and 14 d p.L***	No dosimetry based	Liver kidneys	PRIOR TO RIT: five chemotherapy courses, including three cycles of anthracycline- or platinum-containing regimens, one cycle of cyclophosphamide (4 to 7 g/m <sup>2</sup> ), and one cycle of cytarabine (12 to 24 g/m <sup>2</sup> ).
Winter [30]	Zevalin	rituximab 250mg/m <sup>2</sup>	relapsed or refractory B-cell NHL	44	Activity escalation: 9 cohort 2.2 MBq/kg 43 MBq/kg	14 days after RIT	90% activities were based on dosimetry and were calculated to deliver cohort-defined radiation-absorbed dose (1 to 17 Gy) to critical organs with three to six patients per cohort.	Liver kidneys	high-dose carmustine, etoposide, cytarabine, and melphalan (BEAM)
Bethge [34]	Zevalin	250 mg/m <sup>2</sup> rituximab before dosimetry and 250 mg/m <sup>2</sup> before therapy	Relapsed or refractory: diffuse large B-cell (n=13), blastic mantle cell (n=2), transformed chronic lymphocytic leukemia (n=4), follicular (n=1)	20	Activity escalation: 22 MBq/kg 10 patients; 30 MBq/kg 10 patients	Allogeneic PBSC were transfused on day 14 p.L***	Dosimetry was done for reasons of radiation safety and not used to calculate administered radiation dose, which was weight based.	RM	reduced intensity conditioning (RIC) using fludarabine, melphalan and alemtuzumab
Wahl [37]	Zevalin	375 mg/m <sup>2</sup> weekly for 4 weeks	Relapsed or refractory: follicular (n=11), transformed or mixed follicular (n=5), mantle cell (n=5), diffuse large B-cell (n=1), others (n=2)	24 (18 proceeded to RIT)	Activity escalation: 14.8 MBq/kg (NO ASCT) and 4 cohorts from 2.46 GBq to 6.26 GBq	NO ASCT first group ASCT @ 10-15 d p.L.***	absorbed dose from 18 to 30.5 Gy to live	Liver	none
<b>I-131-MoAbs</b>									
Liu [49]	Bexxar	Tositumomab	small lymphocytic (n=2), diffuse large-cell (n=2), immunoblastic (n=1), diffuse small cleaved-cell (n=3), follicular large-cell (n=4), follicular small cleaved-cell (n=13), follicular mixed small cleaved- and large-cell (n=4)	29	range 10.4 - 29 GBq	N.A.	< 31 Gy to critical organs	Lung kidneys	none
Gopal [26]	Bexxar	-	relapsed or refractory mantle cell lymphoma	16	Range 12-30 GBq	@ 14 days after therapy o radiation exposure < 0.02 mSv/h at 1 m	131I was calibrated to deliver 20 to 25 Gy to vital normal organs.	not reported	10 days later by administration of high-dose etoposide (30-60 mg/kg), cyclophosphamide (60-100 mg/kg)
Gopal [39]	Bexxar	-	relapsed follicular lymphoma	27	Range 10.4-29.1 GBq	@ radiation exposure was less than 0.02 mSv/h at 1 m (RANGE 12-27 DAYS)	131I was calibrated to deliver 20 to 25 Gy to vital normal organs.	Lung kidneys	Two groups: - HD-RIT + ASCT - conventional HD chemotherapy + ASCT
Gopal [27]	Bexxar	-	Relapsed: diffuse large B-cell (n=9), mantle cell (n=8), follicular (n=6), marginal zone (n=1)	24	Range 12.1 - 42.7 GBq	ASCT @ 16 d p.L***	< 25 to 27 Gy to critical organs	Lung liver kidneys	none
Hohloch [33]	131I-rituximab	rituximab 2.5 mg/kg	Relapsed or refractory: follicular (n=4), transformed follicular (n=6), diffuse large B-cell (n=4), mantle cell (n=1), marginal zone (n=1)	16 (9 proceeded to RIT)	median 9 GBq (range 8.6 - 13 GBq)	18-22 days.	Therapeutic activity was calculated according to the protocol in order to obtain a myeloablative dose to the bone marrow and to keep the kidney and lung doses lower than 25 Gy	Lung kidneys	Hexa-BEAM+ BEAM
Wagner [35]	131I-rituximab	rituximab 2.5 mg/kg	Relapsed or refractory: follicular (n=14), marginal zone (n=1), mantle cell (n=5), aggressive B-cell lymphoma (n=3)	23	7.0-19.4 GBq, according to previous dosimetric study planning	@ body activity < 0.22GBq (median of 21 days)	Phase I dose-escalation study including 16 pts: 4 cohorts of 4 pts by level: 21, 23, 25 and 27 Gy to the kidney; 7 pts were treated in the Phase II study on the 27 Gy level.	Kidneys	Three groups: - HD-RIT+ASCT alone -HD-RIT+ASCT+ (EAM + RIT+ASCT) -HD-RIT+ASCT + (BEAM + ASCT) = TANDEM
Gopal [28]	Bexxar	-	relapsed or refractory B-NHL or mantle cell lymphoma	36	median 17.4 GBq; range 9.6 to 59.9 GBq	@ radiation exposure < 0.02 mSv/h at 1 m. (Range 12 -18 days)	absorbed dose of 27 Gy to the critical normal organ	Lung, liver, kidneys	Fludarabine was escalated from 10mg/m <sup>2</sup> daily × 5 days (total dose 50mg/m <sup>2</sup> ) to 30mg/m <sup>2</sup> daily × 7 days (total dose 210mg/m <sup>2</sup> ) without observation of a DLT.
Cassaday [90]	Bexxar	-	mantle cell lymphoma	61	median of 19.8 GBq (range: 7.6-40.7 GBq)	not reported	in order to median 25 Gy (20-27 Gy) to critical organs	not reported	TBI in combination with chemotherapy (high-dose cyclophosphamide with or without etoposide).
Chow [36]	Bexxar	tositumomab 450 mg	relapsed or refractory NHL	107	20.6 GBq (range 6.2 - 36.5)	@radiation exposure ≤0.02 mSv/h at 1 m. (Range 7-13 days)	≤25Gy at critical organs	Lung, liver, kidneys	chemotherapy with etoposide and cyclophosphamide

ACRONYMS: RIT=radioimmunotherapy; HD=high dose; ASCT= autologous stem cell transplantation; RM=red marrow;  
TBI = Total Body Irradiation  
FANDEM = protocol combining HD-chemotherapy + ASCT and HD-RIT + ASCT;  
BEAM = carmustine, etoposide, cytarabine and melphalan chemotherapy; DLT = Dose Limiting Toxicity.

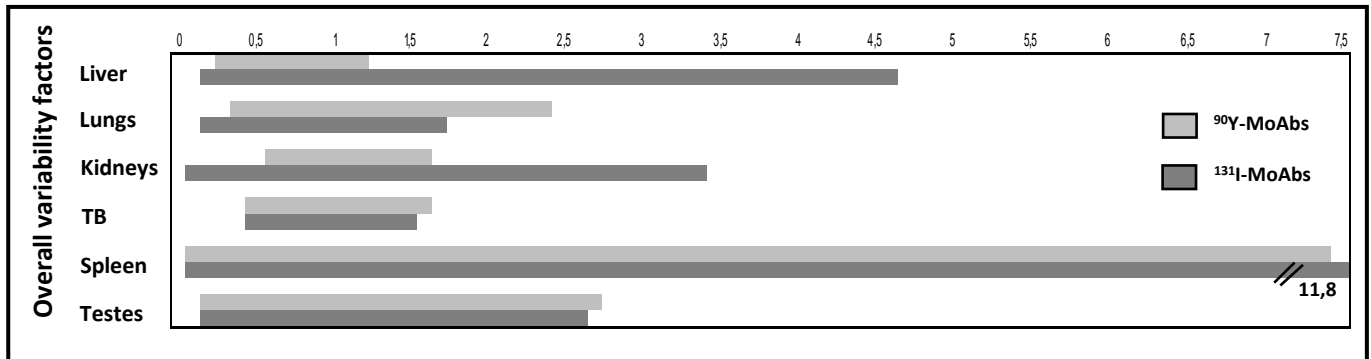


Table 2. Summary of the preivisional dosimety methods used by different authors for NHL RIT. The first four studies concern standard approaches with dosimetry for RM . The other studies refer to hight activity treatments associated with ASCT							
AUTHOR [ref]	TREATMENT	RADIOPHARMACEUTICAL FOR PREVISIONAL DOSIMETRY [INJECTED ACTIVITY]	DOSIMETRY METHODS				RESULTS
			Other Organs		Red Marrow		
Sgouros [64]	RIT	---	Not performed	---	Model 1) Blood-based 2) Marrow biopsy	No RM uptake	"Blood -based model": Equation for red marrow-to-blood activity concentration ratio. Correction factors for red marrow biopsies.
Wiseman [58]	RIT	111In-Ibritumomab tiuxetan [185 MBq]	Planar @ 4–6 h, 1 d, 3 d, 6 d	Corrections: A (a same value for all organs), OM	1) Blood-based 2) Image-based: sacral	Possible RM uptake supposed uniform and checked with method 2	Both dosimetric and pharmacokinetic parameters were unable to predict observed hematologic toxicity
Ferrer [68]	RIT	111In-epratuzumab [120MBq]	Planar @ 1, 4, 24, 48 and 120 h	Corrections: A, S, B, GM	1) Blood-based 2) Image-based: L2-L4	Hypothesis of uniform RM uptake (method 2) or no uptake (method 1)	Only method 3 provides for bone marrow involvement and it better predict hematological toxicity as compared with 1 and 2.
Sgouros [73]	RIT	131I-labeled HuM195 (Anti-CD33) antibody [300 MBq]	Planar @ day of injection, 1 and 2 d post injection	Corrections: A, B, GM	Image-based: - L3-L4 - femoral head - humerus head	Study of regional variability of RM uptake	Large inter- and inpatient variability in marrow total dose. Dosimetry based on a single-site activity concentration measure may not properly estimate marrow toxicity.
Ferrucci [31] Cremonesi [56]	HD-RIT + ASCT	111In-Ibritumomab tiuxetan [185 MBq]	Planar @ 0, 1, 16, 24, 96 and 144 h	Corrections: A, S, B, GM, HCT, OM	Blood-based	Hypothesis of no specific RM uptake	Liver main critical organ and method 3 identified erroneous organs as critical. Individual dosimetry minimizes error sources. Choice of fitting curve crucial in dose calculations. Large inter-patient variability.
Pacilio [41]	RIT/HD-RIT	111In-Ibritumomab tiuxetan [185 MBq]	Planar @ 15 min, 1 h, 8 h, 24 h, 48 h, 72 h, 96 h and 120 h	Corrections: A, B, S, GM, OM	Blood-based	Hypothesis of no RM uptake	Liver, lung and kidney main organs at risk. Strong disagreement in dose results with Cremonesi/Ferrucci et al. [23,33] and with Wiseman et al. [53] works. Better agreement with Devizzi/Chiesa et al. [24,51].
Devizzi [32] Chiesa [57]	HD-RIT + ASCT	111In-Ibritumomab tiuxetan [median: 200 MBq]	Planar @ 0–1, 18–26, 40–48, 120–140 h	Corrections: A, B, S, GM, HCT, OM	1) Blood-based 2) Image-based in 3 patients: -sacrum -humerus -L2,L3,L4	RM uptake/uniformity checked with method 2	Large inter-patient variability. Fixed-activity approach does not properly exploit the possibility of the treatment. Disagreement between RM dose estimations with method 1) and 2) and between L2-L4 and the other ROIs. No evident correlation between RM absorbed dose and platelet reduction.
Wahl [37]	HD-RIT + ASCT	111In-Ibritumomab tiuxetan [185 MBq]	Hybrid method: planar @ 0–1, 4, 24, 72, and 144 h + SPECT/CT @ 24 h	Corrections: A, B, S, OM	1) Blood-based 2) Image-based	Details not specified	Liver main organ at risk, but RM dose crucial for ASCT timing. MTD to liver seems to exceed 28 Gy. Large inter-patient variability. Hybrid approach is feasible for organ dosimetry-based HD-RIT with ASCT.
Hohloch [33]	TANDEM	131I-rituximab [370-400MBq]	Planar @ 1 h - 8 days	Corrections: GM, others not specified	Blood-based	Hypothesis of no RM uptake	Lungs and kidneys dose-limiting organs.
Gopal [28]	HD-RIT + fludarabine + ASCT	131I-tositumomab [185-370MBq]	Planar @ day of injection, 48, 96, and 120 h post injection	Corrections: A, B, GM, OM	Image-based	Details not specified	Lungs, liver and kidneys main critical organs.
Chow [36]	HD-RIT + HD chemotherapy + ASCT	131I-tositumomab [1.7mg/kg or 35mg] + unlabelled tositumomab [450mg]	Planar @ day of injection, 48, 120, 144 h post injection	Corrections: A, B, S, GM, OM	Not specified	Not specified	Lungs, liver and kidneys main critical organs.
Winter [30]	RIT (dose escalation) + HD-BEAM + ASCT	111In-Ibritumomab tiuxetan [185 MBq]	Planar @ 0, 4, 24, 72 and 144 h post injection	Corrections: A (a same value for all organs), OM	Not specified	Not specified	Large inter-patient variability underscores the importance of careful dosimetry evaluations. A dosimetry-based approach, rather than a weight-based approach, is recommended to safely deliver the highest possible dose. Liver and kidneys main critical organs.

ACRONYMS: RIT=radioimmunotherapy; HD=high dose; ASCT= autologous stem cell transplantation; RM=red marrow; A=attenuation; B=background; S=scattering; GM=geometric mean; OM=organ masses; HCT=hematocrit; MTD=maximum tolerated dose; TANDEM = protocol combining HD-chemotherapy + ASCT and HD-RIT + ASCT; BEAM = carmustine, etoposide, cytarabine and melphalan chemotherapy.

**Table 3.** Ranges of variability factors related to the absorbed doses to normal organs, normalised to the median absorbed dose values.

Reference		n. pts	Liver	Lungs	Kidneys	TB	Spleen	Testes
<b><sup>131</sup>I-MoAbs</b>	Kaminski <sup>90</sup>	7	0.8 - 1.3	0.7 - 1.9	0.7 - 1.6	0.6 - 1.2	0.4 - 1.8	- .
	Gopal <sup>27</sup>	24	0.6 - 1.2	0.6 - 1.2	0.6 - 1.4	0.7 - 1.5	0.3 - 1.8	-
	Hattori <sup>91</sup>	67	0.3 - 1.2	0.4 - 1.2	-	0.6 - 1.5	0.1 - 7.4	0.2 - 2.7
	Chow <sup>36</sup>	107	-	0.4 - 2.4	-	0.5 - 1.6	-	-
	Hohloch <sup>33</sup> *	9	-	0.6 - 1.2	0.6 - 1.2	-	-	- .
<b><sup>90</sup>Y-MoAbs</b>	Wiseman <sup>58</sup>	229	0.2 - 4.5	0.2 - 1.7	0.1 - 3.3	0.6 - 1.5	0.1 - 3.0	0.3 - 1.5
	Delaloye <sup>93</sup>	57	0.3 - 2.4	0.5 - 2.4	0.5 - 2.7	0.6 - 1.5	0.4 - 2.3	-
	Cremonesi <sup>56</sup>	22	0.5 - 2.8	0.2 - 1.6	0.2 - 2.0	0.5 - 1.1	0.3 - 2.3	0.2 - 2.6
	Chiesa <sup>57</sup>	15	0.7 - 1.4	0.7 - 1.4	0.5 - 1.3	-	0.7 - 1.4	0.5 - 1.7
	Whal <sup>37</sup>	18	0.5 - 1.6	0.5 - 1.6	0.6 - 1.5	-	0.5 - 11.8	-
	Bethge <sup>34</sup>	18	0.2 - 1.9	0.2 - 5.2	0.4 - 3.4	-	0.3 - 3.0	-



Note: For each organ, the variability factors are defined as the following ratios: min/median absorbed dose value, and maximum/median absorbed dose value. Thus, indicating with X the median value of the absorbed dose to an organ, for a range of variability factors e.g. 0.4 – 3.2, the range of the absorbed doses for a same activity administered is: (0.4·X, 3.2·X).

\* Study on <sup>131</sup>I-Rituximab.